The response of calcareous nannoplankton to Oceanic Anoxic Events: The Italian pelagic record.

Elisabetta Erba*, Cinzia Bottini, Giulia Faucher, Gabriele Gambacorta, Stefano Visentin

E. Erba, Università degli Studi di Milano, Dipartimento di Scienze della Terra "Ardito Desio", Via Mangiagalli 34, 20133 Milano, Italy, elisabetta.erba@unimi.it, * Corresponding Author
C. Bottini, Università degli Studi di Milano, Dipartimento di Scienze della Terra "Ardito Desio", Via Mangiagalli 34, 20133 Milano, Italy, cinzia.bottini@unimi.it,
G. Faucher, Università degli Studi di Milano, Dipartimento di Scienze della Terra "Ardito Desio", Via Mangiagalli 34, 20133 Milano, Italy, giulia.faucher@unimi.it,
G. Gambacorta, Università degli Studi di Milano, Dipartimento di Scienze della Terra "Ardito Desio", Via Mangiagalli 34, 20133 Milano, Italy, gabriele.gambacorta@guest.unimi.it,
S. Visentin, Università degli Studi di Milano, Dipartimento di Scienze della Terra "Ardito Desio", Via Mangiagalli 34, 20133 Milano, Italy, stefano.visentin@unimi.it

KEYWORDS: Oceanic anoxic events, calcareous nannofossils, paleoecology, Italian pelagic sections

ABSTRACT

The Earth history is punctuated by cases of extreme global stress of concurrent warming, ocean fertilization and acidification that impacted biologic diversity and functioning. Under excess CO_2 and greenhouse conditions, the Mesozoic deep ocean became temporarily depleted of oxygen, promoting the accumulation of massive amounts of organic matter during Oceanic Anoxic Events (OAEs). Although global anoxia and enhanced organic matter burial are the most striking and intriguing paleoceanograhic phenomena, OAEs can be studied also to decipher the oceanic ecosystem response to CO_2 pulses. In Jurassic and Cretaceous oceans, calcareous nannoplankton were already common from coastal to open oceanic settings and of enough abundance and diversity to produce calcareous oozes. Indeed, Jurassic and Cretaceous pelagic micrites mainly consist of coccoliths and nannoliths, in addition to variable amounts of diagenetic carbonate. Therefore, pelagic limestones are ideal for epitomizing variations in abundance and composition of calcareous

phytoplankton and, consequently, of primary producers at large scale to understand their response to global change.

Italian pelagic successions are a reference for the Tethys Ocean and, in general, for low to middle latitudes. We consider here well-dated sections with quantitative nannofossil data across OAEs to synthetize changes in abundance of the dominant, micrite-forming, nannofossil taxa and species-specific variations in size to trace the response of calcareous nannoplankton as expressed by biocalcification across the early Toarcian T-OAE, late Valanginian Weissert-OAE, early Aptian OAE1a and latest Cenomanian OAE2. In general, a major decrease in nannofossil abundance is recorded for the highly calcified dominant forms, evidenced by the "*Schizospaherella* crisis", the "nannoconid decline" and the "nannoconid crisis" during the T-OAE, Weissert-OAE and OAE1a, respectively. An even more dramatic drop in coccolith/nannolith abundance characterizes OAE2, with a nannoplankton biocalcification "blackout" through the Bonarelli Level in Italian sections. Despite these abundance crises, calcareous nannofloras recovered soon after the paleoenvironmental perturbation terminated, although the return to pre-OAE conditions occurred rather slowly and assemblage composition renewed to a different state. Species-specific changes in size were detected for *Schizosphaerella* across the T-OAE and for *B. constans* in the intervals of maximum perturbation within OAE1a and OAE2. Size of *N. steimannii*, conversely, does not show variations across the Weissert-OAE and OAE1a.

The T-OAE and OAE1a were preceded and accompanied by a few millions-years long origination phase, indicating the calcareous nannoplankton ability to positively respond and overcome stressing oceanic conditions, as further evidenced by absence of extinctions. Calcareous nannoplankton reacted differently during the Weissert-OAE and OAE2 as the Valanginian "nannoconid decline" is gradual and followed by a symmetric increase in abundance, while the late Cenomanian nannofossil drop in abundance was as sudden as its recovery. In both cases, extinctions are paralleled by entry of new taxa, at a slower rate across the Weissert-OAE and at faster rates in the case of OAE2. While the influence of paleoenvironmental stress on calcareous nannofloral abundance and composition during the early Toarcian T-OAE, late Valanginian Weissert-OAE, early Aptian OAE1a and latest Cenomanian OAE2, are clearly recorded in Italian pelagic sections and at supra-regional to global scale, the role of OAE pressure on nannoplankton evolution, if any, was differentiated and resulted in overall originations. Calcareous nannofossil patterns underline the resilience of this phytoplankton group during OAE perturbations.

RIASSUNTO

La storia della Terra è punteggiata da eventi di stress globale estremo evidenziato da riscaldamento, fertilizzazione e acidificazione oceanica che hanno influito sulla diversità e sul funzionamento del biota marino. In condizioni di eccesso di CO_2 e di clima a effetto serra, durante il Mesozoico i fondali marini hanno sperimentato temporanea anossia e accumulo di materia organica durante eventi anossici oceanici (OAE). Sebbene l'anossia globale e il seppellimento di grandi quantità di C organico siano i fenomeni paleoceanografici più intriganti, gli OAE possono essere studiati anche per decifrare la risposta dell'ecosistema oceanico a perturbazioni globali. Negli oceani del Giurassico e Cretacico, il nannoplancton calcareo era già diffuso dalle zone costiere all'oceano aperto, in sufficiente abbondanza e diversità per produrre sedimenti biogenici calcarei. Infatti, le micriti pelagiche del Giurassico e del Cretacico consistono principalmente di coccoliti e nannoliti, oltre a quantità variabili di carbonato diagenetico. Pertanto, i calcari pelagici sono ideali per quantificare le variazioni di abbondanza e composizione del fitoplancton calcareo e, di conseguenza, dei produttori primari per comprenderne la risposta ai cambiamenti globali.

Le successioni pelagiche italiane sono considerate di riferimento per l'Oceano della Tetide e, in generale, per le basse-medie latitudini. In questo lavoro, abbiamo considerato sezioni stratigrafiche ben datate e con dati quantitativi delle associazioni a nannofossili calcarei, per sintetizzare i cambiamenti in abbondanza dei taxa dominanti e delle variazioni dimensionali di alcune specie al fine di tracciare la risposta del nannoplancton calcareo tramite la biocalcificazione durnate il T-OAE del Toarciano inferiore, il Weissert-OAE del Valanginiano superiore, l'OAE1a dell'Aptiano inferiore e l'OAE2 del Cenomaniano sommitale. In generale, si registra una drastica diminuzione dell'abbondanza dei nannofossili, soprattutto per le forme dominanti altamente calcificate, come evidenziato dalla "crisi di *Schizospaherella*", dal "declino dei nannoconidi" e dalla "crisi dei nannoconidi" durante i T-OAE, Weissert-OAE e OAE1a, rispettivamente. Una riduzione ancora più drammatica dell'abbondanza di coccoliti/nannoliti caratterizza l'OAE2, con un "blackout" della biocalcificazione del nannoplancton durante la deposizione del Livello Bonarelli nelle sezioni italiane. Nonostante queste crisi di abbondanza, le nannoflore calcaree si sono ristabilite subito dopo la fine della perturbazione paleoambientale, sebbene il ritorno a condizioni pre-OAE sia avvenuto piuttosto lentamente e le associazioni abbiano raggiunto una composizione diversa. Sono stati rilevati cambiamenti delle dimensioni di *Schizosphaerella* attraverso il T-OAE e di *B. constans* negli intervalli di massima perturbazione all'interno degli OAE1a e OAE2. Le dimensioni di *N. steimannii*, al contrario, non mostrano variazioni durante il Weissert-OAE e l'OAE1a.

Il T-OAE e l'OAE1a sono stati preceduti e accompagnati da una fase di speciazione del nannoplancton, durata alcuni milioni di anni, che indica la capacità del fitoplancton calcareo a rispondere positivamente superando condizioni oceaniche stressanti, come evidenziato anche dall'assenza di estinzioni. Il nannoplancton calcareo ha reagito in modo diverso durante il Weissert-

OAE e l'OAE2 poiché il "declino dei nannoconidi" del Valanginiano è graduale e seguito da un altrettanto graduale aumento dell'abbondanza, mentre la riduzione dei nannofossili nel Cenomaniano sommitale è stata repentina come il suo recupero. In entrambi i casi, si sono verificate alcune estinzioni ma contemporaneamente anche la speciazione di nuovi taxa, a un ritmo più lento attraverso il Weissert-OAE e a tassi più rapidi nel caso dell'OAE2.

Mentre l'influenza dello stress paleoambientale sull'abbondanza e composizione delle nannoflore calcaree durante il T-OAE, il Weissert-OAE, l'OAE1a e l'OAE2 è chiaramente registrata nelle sezioni pelagiche italiane e spesso su scala sopra-regionale fino a globale, l'influenza degli OAE sull'evoluzione del nannoplancton, se causale, è stata differenziata e ha generalmente indotto delle speciazioni. Le variazioni riscontrate nelle associazioni a nannofossili calcarei sottolineano la resilienza di questo gruppo di fitoplancton durante le perturbazioni ambientali associate agli OAE.

INTRODUCTION

The early phase of the Deep Sea Drilling Project provided evidence of extensive occurrence of Cretaceous black shales from previously unsampled oceanic basins. As on-land, stratigraphies of pelagic successions showed that organic carbon-rich lithologies are confined to specific geologically short intervals suggesting a global rather than local to regional oxygen-depletion of bottom waters.

The term "Oceanic Anoxic Event" (OAE) was coined by Schlanger & Jenkyns (1976) after the recovery of mid-Cretaceous black shales at sites drilled in the Pacific Ocean. Such lithologic units were recognized as equivalent and coeval of well-known lithostratigraphic markers previously described in the Tethys and Atlantic Oceans. The term OAE was originally defined to signify time intervals during which black shale deposition was prevalent at a global scale. The original definition was, therefore, based on lithologic criteria and applied to two time intervals, namely the Aptian-Albian (OAE1) and the Cenomanian-Turonian (OAE2). Later investigations on land and in the oceans pointed out the occurrence of the Coniacian–Santonian OAE3 (Arthur & Schlanger, 1979; Jenkyns, 1980) and of the Toarcian OAE (Jenkyns, 1985, 1988). Based on integrated and higher resolution stratigraphy, Arthur et al. (1990) subdivided OAE1 into discrete events OAE1a, OAE1b, OAE1c and OAE1d, still using the sedimentary record of organic C-rich black shales.

The most spectacular sedimentary expression of the early Aptian and latest Cenomanian events are the Livello Selli and Livello Bonarelli, respectively. For both the type area is the Umbria-Marche Basin (central Italy), where a continuous pelagic succession deposited in the Jurassic to Paleogene interval. The first event that was recognized and the most studied is the Bonarelli Level, named after its discoverer Guido Bonarelli. In fact, in 1891 Bonarelli described "*uno strato di scisto*

nero bituminoso" (a level of black organic-rich shale), about 1 meter thick, in the uppermost part of the Scaglia Bianca in the region of Gubbio, close to the Cenomanian/Turonian boundary (Fig. 1).

At the beginning of the XX century, Dal Piaz (1907) described Toarcian organic-rich facies in pelagic Jurassic successions of the Alpi Feltrine in the Southern, similarly to other occurrences in Germany and Switzerland (Posidonienschiefer), England (Jet Rock and Bituminous Shales) and France (Schistes Cartons). Dal Piaz's perception of black shales as geological archives of major environmental changes was by far innovative and a precursor of modern paleoceanography. A few decades later Gaetani & Poliani (1978) described a lower Toarcian black shale interval, named "*Livello a Pesci*" (Fish Level), in the pelagic succession of the Lombardy Basin (Fig. 1). In the 80s, Jenkyns (1985, 1988) labelled these black shale intervals as the Toarcian OAE (T-OAE).

The identification of the Livello Selli is much younger (Coccioni et al., 1987) and, again, was based on the occurrence of a 1-3 m thick marker bed described as a "*livello radiolaritico-bituminoso-ittiolitico*" (a black shale interval enriched in radiolarians, fish remains and organic matter) in the lowermost part of the Marne a Fucoidi Formation through the Umbria-Marche Basin (Fig. 1).

With the rapid development of chemostratigraphy, and specifically of C and O stable isotopic investigations, it became clear that the T-OAE, OAE1a and OAE2 are associated with negative and positive anomalies of carbon-isotope curves obtained from carbonate and/or organic matter, caused by major perturbations of the global carbon cycle (Jenkyns, 2010). The original definition of OAEs (Schlanger & Jenkyns, 1976) has become somehow misleading for various reasons: a) anoxia is rarely reached; b) terrestrial successions also record the global C cycle anomalies; c) anomalies are of long to short duration; d) black shale intervals were proved to be diachronous in many cases.

High-resolution integrated stratigraphy of marine and terrestrial records has produced a solid time framework for OAEs (Robinson et al., 2017), and $\delta^{13}C$ chemostratigraphy has grown as a prominent basic tool for identifying, characterizing and correlating OAEs (e.g. Erba, 2004; Tsikos et al., 2004; Weissert & Erba, 2004; Jenkyns, 2010). In fact, although a black marker bed is not present in Lower Cretaceous pelagic successions (Fig. 1), a discrete C isotope excursion of late Valanginian age was identified in the Maiolica Formation from the Southern Alps (Weissert, 1989; Lini et al., 1992). Such an anomaly was constrained by bio-magnetostratigraphy (Channell et al., 1993) and used by Erba et al. (2004) to formalize the Valanginian event as the "Weissert OAE". Global anoxia has not been documented, but discrete black shale levels enriched in organic matter are described from the Tethys and Pacific Oceans in the early phase of the Weissert-OAE (Erba et al., 2004).

In the past four decades OAEs have been recognized in oceanic and terrestrial sequences, highlighting local variations in depositional conditions, various types and degrees of diagenesis, and preservation of organic matter. As summarized by Jenkyns (2010), equivalents of the Bonarelli,

Selli, Weissert and Toarcian events have been recognized in a variety of sedimentary basins, and a number of geochemical anomalies have been detected in addition to C isotopic excursions. Yet, a lively debate about causes and consequences of OAEs and their influence on biota continues to involve experts from various disciplines within geosciences. The original hypotheses of Schlanger & Jenkyns (1976) are still discussed to discern and discriminate the role of productivity from that of organic matter preservation under anoxic conditions. Pelagic successions containing OAEs are crucial to understand the biotic variations in marine planktonic communities associated with such global perturbations of the ocean/atmosphere system. In marine ecosystems coccolithophores are part of phytoplankton responsible for primary productivity, energy transfer to higher trophic levels, export of biogenic particles to the seafloors and exchanges between the surface ocean and the atmosphere. The term calcareous nannoplankton was originally introduced by Lohman (1909) for planktonic organisms smaller than 63 μm and is now used for golden-brown algae coccolithophores (phylum Haptophyta) secreting tiny calcite crystals to build coccoliths and ultimately coccospheres. The global occurrence of calcareous nannoplankton and their biomineralization make these phytoplanktonic algae a most effective producers of calcite on Earth. Calcareous nannofossils include the fossil remains of coccolithophores, namely coccoliths and coccospheres as well as associate nannoliths often of unknown provenance.

In Jurassic and Cretaceous oceans, calcareous nannoplankton was already the most efficient rock-forming group (e.g. Erba 2006). Indeed, Jurassic and Cretaceous pelagic micrites mainly consist of coccoliths and nannoliths, in addition to variable amounts of diagenetic calcite. Consequently, pelagic carbonates offer the opportunity of characterizing variations in abundance and composition of calcareous nannofloras across OAEs to quantify their resilience to extreme conditions.

Italian pelagic successions represent excellent records of the Tethys Ocean (Figs. 1 and 2) and, in fact, have been studied for a long time. The first documentations of nannofossil-rich limestones were based on scanning electron microscope investigations of Maiolica and Scaglia limestones (Farinacci, 1964). These pioneering studies unequivocally demonstrated the rock-forming role of calcareous nannoplankton as further discussed by Noël & Busson (1990) also for Jurassic pelagic successions of the Tethys. Indeed, it became clear that *Schizospaherella* and *Nannoconus* can reach high abundances in pelagic and hemipelagic carbonates of Jurassic and Cretaceous age. The name "nannoconite" was proposed for *Nannoconus*-limestone (Bréhéret, 1983) and quantitative studies conclusively showed that Lower Cretaceous Maiolica limestones are nannoconites (Erba, 1994; Erba & Tremolada 2004). Similarly, *Schizosphaerella* can be so abundant (e.g.: Kälin & Bernoulli, 1984; Claps et al., 1995; Mattioli, 1997; Erba, 2004; Casellato & Erba, 2015; Peti & Tibault, 2017) as to produce a “schizosphaerellite”.

Quantitative studies of Cretaceous pelagic successions, comprising OAEs, reveal major shifts in the biogenic component: from carbonate-dominated to siliceous- and organic matter-dominated (Premoli Silva et al.,1999; Leckie et al., 2002; Erba, 2004). Usually, calcareous nannofossils are abundant below and above black shales representing OAEs, when radiolarians and organic-walled microorganisms become overwhelming. The nannofossil record, in fact, traces major decreases in abundances across the perturbation, especially of the dominant forms that usually show incomplete recovery after termination of OAEs (Erba, 2004).

Erba (2004) reviewed changes in calcareous nannofossil assemblages across the T-OAE, OAE1a and OAE2 and proposed paleoceanographic and paleoecologic dynamics. In this work, we focus on calcareous nannofossil changes across OAEs recorded in pelagic Italian successions that are, still, reference records of global changes at low to middle latitudes. Our synthesis regards only well-dated sections with quantitative nannofossil data and $\delta^{13}C$ chemostratigraphy for the T-OAE, Weissert-OAE, OAE1a and OAE2. In particular, for each OAE we will highlight changes in abundance of the dominant (micrite-forming) nannofossil taxa and species-specific variations in size to trace the response of calcareous nannoplankton via biocalcification.

MATERIAL AND METHODS

Fig. 3 reports on map the locations of the sections considered for this work and the paleogeography of the Tethyan area during the Jurassic-Cretaceous interval is shown in Fig. 2. Considered sections mostly lie in the Southern Alps (sections 1 to 14) and the Umbria-Marche Basin (sections 15 to 27), but a few key-successions were studied in the Gargano area (section 28), Sicily (sections 29 to 31) and Sardinia (section 32). The sedimentary expression of the T-OAE, Weissert-OAE, OAE1a and OAE2 on Italian key-sections is illustrated in Fig. 1. A summary of the papers documenting calcareous nannofossil quantitative and morphometric data and C isotopic characterization of the T-OAE, Weissert-OAE, OAE1a and OAE2 is reported in Tabs. 1, 2, 3 and 4, respectively.

We selected all published papers with available quantitative nannofossil data from Italian pelagic sections and/or C_{carb} and C_{org} stable isotope data for the early Toarcian T-OAE, the late Valanginian Weissert-OAE, the early Aptian OAE1a and the latest Cenomanian OAE2. The data are summarized in a graphical form by reporting as bars the relative stratigraphic range of each section, separately for nannofossil and C isotopic data. In case the same section was described in multiple papers, we synthesized in a single bar the cumulative extent of the data generated for the analyzed stratigraphic interval (Tabs. 1, 2, 3 and 4). The presence and extension of hiatuses are also reported. The resulting synthesis figures are intended to help the reader in rapidly identifying the

relevant literature and have an overall framework of C isotopic chemostratigraphy applied to Jurassic and Cretaceous OAEs in Italian sections.

As previously discussed, the operational definition of OAEs has partially changed, and various authors based OAE boundaries (onset and termination) on lithostratigraphic or chemostratigraphic data. In most cases biostratigraphy was used to constrain age attribution and possibly identify/confirm hiatuses eliding part of the OAEs. It should also be stressed that in many cases black shales are diachronous, disavowing the original definition of Schlanger & Jenkyns (1976). The definitions adopted in this paper are as follows:

* the **T-OAE** corresponds to the negative excursion in the carbonate and organic carbon isotope profile (Jenkyns, 2010);

* the **Weissert-OAE** is based on the $\delta^{13}C$ curve: its beginning and end are placed at the base of the positive excursion and its climax, respectively (Erba et al., 2004);

* the early Aptian **OAE1a** corresponds to the Selli Level. With reference to the $\delta^{13}C$ chemostratigraphy, the onset coincides with the sharp decrease of the negative shift (C3-Ap3) and terminates at the base of the extended positive excursion named C7-Ap7 (Menegatti et al., 1998; Bottini et al., 2015);

* the latest Cenomanian **OAE2** is based on the $\delta^{13}C$ curve: its beginning and end are placed at the base of the positive excursion and its climax, respectively (Tsikos et al., 2004).

As discussed by Jenkyns (2010), the amplitude of carbon isotope anomaly is usually greater in marine and terrestrial organic matter than in carbonate. However, when bulk $\delta^{13}C_{carb}$ chemostratigraphy is considered, values are most repetitive in many marine sections, allowing the construction of reference synthesis curves (e.g. Erba, 2004; Weissert & Erba, 2004: Jarvis et al., 2006; Robinson et al., 2017; Bottini & Erba, 2018) (Fig. 3).

As far as Italian sections are concerned, (semi)quantitative analyses of nannofossil abundances of Lower Jurassic (T-OAE) and Lower Cretaceous intervals (Weissert-OAE and OAE1a) were performed on ultrathin sections by light polarizing microscope at 1250X magnification. Thin sections were thinned to an average thickness of 7 μm in order to have an adequate view of nannofloras, and nannofossil absolute abundances were gained counting all specimens in 1 mm^2 (Erba, 1994, 2004; Erba & Tremolada, 2004; Bottini et al., 2015; Casellato & Erba, 2015). For the OAE2 interval, total nannofossil abundances were obtained on simple smear slides: the nannofossil assemblages were quantified by counting at least 300 specimens in each sample using a light polarizing microscope at 1250X magnification; the total abundance was calculated as the average number of nannofossils per field of view (Erba, 2004).

In addition to trends of nannofossil abundances, we report here species-specific changes in size of selected taxa across the T-OAE, Weissert-OAE, OAE1a and OAE2. Particularly, morphometric investigations were applied to gather size fluctuations of: a) *Schizosphaerella* across the T-OAE; b) *Nannoconus steinmannii* across the Weissert-OAE; c) *N. steinmannii* and *Biscutum constans* across OAE1a; d) *B. constans* across OAE2. Size measurements were carried out on simple smear slides. Morphometry of *Schizosphaerella* and *B. constans* is based on digital photographs acquired with a camera mounted on a Leitz Laborlux light microscope and using the ImageJ64 software. Morphometric analyses of *N. steinmannii*, instead, were obtained with built-in camera Olympus DP73 set on the light microscope Leica DM2700P and using the Fiji software (Schindelin et al., 2012).

Schizosphaerella specimens were measured taking into account the maximum diameter of the valve (Fig. 4), similarly to Mattioli & Pittet (2002). *N. steinmannii* is shaped like an elongated frustum of cone, and measured parameters include the maximum width (base width), the minimum width (top width) and the height (Fig. 4). In addition, the volume of each specimen was calculated. Coccoliths of *B. constans* are elliptical in shape, consequently length and width were measured for individual specimens (Fig. 4).

NANNOFOSSIL ABUNDANCE AND SIZE CHANGES ACROSS OAEs

Previous papers documented variations in nannofossil assemblage composition related to paleotemperature and paleofertility fluctuations and nannofossil indices were reconstructed prior, during and after OAEs recorded in Italian sections (Erba, 2004; Casellato & Erba, 2015; Bottini et al., 2015; Bottini & Erba, 2018). In this chapter we synthetize and discuss the changes in calcareous nannofossil abundance and coccolith/nannolith size as potential proxies of biocalcification adjustments under altered oceanic carbonate chemistry. Data are presented in stratigraphic order from the oldest to the youngest OAE.

The Toarcian T-OAE

A total of nine Italian pelagic sections cover the T-OAE (Fig. 5): the Val Ceppelline, Colle di Sogno and Brasa sections in the Lombardy Basin, the Dogna section in the Belluno Basin, the Valdorbia, Colle d'Orlando, Pozzale, Somma and Fonte Cerro sections in the Umbria-Marche Basin. Six out of the nine sections were investigated for carbon isotope chemostratigraphy, while for three sections the identification of the stratigraphic position of the T-OAE was based on biostratigraphy. As summarized in Tab. 1, a limited amount of papers documents the occurrence of the Toarcian C isotopic anomaly in Italian sections. In particular, it is important to stress that for the Val Ceppelline and Colle di Sogno section nothing was published in recent years, as the only C isotopic data were

presented by Jenkyns & Clayton (1986). The Dogna (Jenkyns et al., 2001) and Valdorbia (Sabatino et al., 2009) sections undoubtedly represent to date the best available Italian record, with a high-resolution comparable to modern standards. We highlight that for the Brasa section in the Lombardy Basin and the Colle d'Orlando and Fonte Cerro sections in the Umbria-Marche Basin, no carbon isotopic data were published.

Quantitative and semiquantitative nannofossil data are available for the Colle di Sogno (Casellato & Erba 2015), Brasa (Cobianchi & Picotti, 2001), Colle d'Orlando, Pozzale, Somma and Fonte Cerro sections (Bucefalo Palliani et al., 1998; Mattioli & Pittet, 2004) (Fig. 5). Morphometric analyses of *Schizosphaerella* are available for the Somma section (Mattioli et al., 2004b, 2009) and were obtained for the Sogno Core (this study) drilled at Colle di Sogno. Quantitative analyses of *Schizosphaerella* and *Mitrolithus jansae* identified changes in abundance of these taxa across the T-OAE (Casellato & Erba, 2015): after a period of stability and oligotrophy which promoted a diversified calcareous phytoplankton community dominated by these rock-forming deep-dwellers (Fig. 5), enhanced nutrient availability under increased run-off, possibly induced the "*Schizosphaerella* decline" detected close to the Pliensbachian/Toarcian boundary, also accompanied by a marked decrease in abundance of *M. jansae* and an increase in abundance of *Biscutum* and *Lotharingius* (Casellato & Erba, 2015). Just before the onset of T-OAE, a further drop in abundance is shown by both *Schizosphaerella* and *M. jansae,* with the exclusion of "encrusted *S. punctulata*" and the survival of "thin *M. jansae*" (Casellato & Erba, 2015). In the Fish Level both *S. punctulata* and *M. jansae* drop in abundance while small coccoliths show an increase in abundance that, however, contributed very little to calcite production, justifying the low carbonate content of the T-OAE black shales at Colle di Sogno (Casellato & Erba, 2015). In the interval above the Fish Level, nannofossils are mostly represented by small taxa with some contribution by *S. punctulata*, while *M. jansae* barely survived the paleoenvironmental stress and disappeared soon after the T-OAE termination (Fig. 5). Indeed, paleoceanographic conditions in the photic zone resumed gradually to a pre-perturbation state, suggesting that the deepening of the nutricline, the re-establishment of stability and of marine carbonate chemistry required an extended period after the end of anoxia (Casellato & Erba, 2015).

The "*Schizosphaerella* crisis" is evidenced by its drastic reduction in abundance just prior to the T-OAE black shale interval and represents the temporary breakdown of such a rock-forming taxon (Erba, 2004; Tremolada et al., 2005). Similar and coeval decreases in abundance of *S. punctulata* - and in general in nannofossil total abundances - are reported from Portugal (Mattioli et al., 2008), Spain (Fraguas et al., 2012), and France (Hermoso et al., 2012) pointing to a major shift in nannofloral assemblages at supra-regional scale.

The T-OAE perturbation also affected the biomineralization of *Schizosphaerella* showing reduced sizes as documented in the Somma section (Mattioli et al., 2004b, 2009). Fig. 6 illustrates

the size changes measured in the Sogno Core (this study) obtained for the interval preceding the T-OAE, within the T-OAE and in samples from the overlying interval. Both the mean and median diameter values decrease in the black shale interval, further evidencing - contemporaneously to the abundance drop - decreased calcification of *Schizosphaerella*. Such decrease in size was also documented in Italy for the Somma section (Mattioli et al., 2004b, 2009), in France (Clemence et al., 2015), Spain (Suan et al., 2010, and Portugal (Suan et al., 2008).

The nannoplankton patterns described above for Italian pelagic sections confirm general trends documented elsewhere indicating stepped paleoenvironmental perturbations culminating into the T-OAE. The extreme conditions resulting from combined warming, ocean fertilization and possibly acidification contributed to the establishment and maintenance of very stressing surface waters with dominance of opportunistic taxa. Ocean acidification might have reached threshold values at the onset of the T-OAE inducing the "*Schizosphaerella* crisis", the drop in abundance of *M. jansae* and the temporary size reduction in *Schizosphaerella.*

Environmental stress started to affect the ocean structure, fertility and chemistry at least 1 million years before the T-OAE, close to the Pliensbachian/Toarcian boundary, that was a time of accelerated nannoplankton speciation, a most spectacular case for calcareous nannoplankton evolution within the Mesozoic (Bown et al., 2004; Erba, 2006). Data from Italian pelagic sections support the interpretation of the T-OAE as a nutrification episode combined with some ocean acidification exerting a direct control on phytoplankton type and abundance, and influencing species-specific biocalcification.

The late Valanginian Weissert OAE

Eight sections covering the Weissert-OAE were analysed for C isotopic chemostratigraphy (Fig. 7). In particular, five sections were studied in the Lombardy Basin (Pusiano, Rio Corna, Capriolo, Polaveno, Valle Aviana sections), while the Valle del Mis and Chiaserna sections are located in the Belluno and Umbria-Marche Basins, respectively. Finally, we also considered here the S'Ozzastru section in Sardinia, although deposited during flooding of a carbonate ramp. Two major papers published in the nineties still represent the sole reference of the Weissert-OAE in Italy (Lini et al., 1992; Channell et al., 1993). However, recent works at the Chiaserna (Sprovieri et al., 2006) and S'Ozzastru sections (Bottini et al., 2018) document with new data the occurrence of the Weissert carbon isotopic anomaly. It should be noticed that not all of these outcrops cover the entire OAE: the Val del Mis section records just the descending trend of the event after the C isotopic anomaly, and the S'Ozzastru section covers the initial increase of the carbon isotopic excursion (Fig. 7).

Calcareous nannofossil absolute abundances were quantified only for the Polaveno section (Erba & Tremolada, 2004), but semiquantitative data are also available for Pusiano section (Channell et al., 1993). The Weissert-OAE interval is marked by a decline in abundance of all nannoconids, called "nannoconid decline'' (*sensu* Channell et al., 1993), whose onset correlates with magnetochron M12 and predates the positive $\delta^{13}C$ excursion. Nannoconid abundance resumes during the C isotopic recovery starting within magnetochron CM10N. The "nannoconid decline'' interval is also characterized by higher abundance of *Diazomatolithus* throughout the entire Weissert-OAE interval. Absolute abundances of *Diazomatolithus* (Erba & Tremolada, 2004) show a symmetric increase and decrease specular to the relative decrease and increase in abundance of nannoconids. In Italian pelagic sections, the onset of the "nannoconid decline" is also marked by a peak in abundance of pentaliths (Bersezio et al., 2002; Erba & Tremolada, 2004) (Fig. 7).

The "nannoconid decline'' depicted in the Tethyan sections (Channell et al., 1993; Bersezio et al., 2002; Erba & Tremolada, 2004; Bottini et al., 2018) was proved as a nannofloral assemblage shift with global significance (Erba et al., 2004; Bornemann & Mutterlose, 2008; Greselle et al., 2011; Barbarin et al., 2012; Duchamp-Alphonse et al., 2014; Mattioli et al., 2014).

Morphometric analyses of *N. steinmannii* were performed for the Polaveno section (Fig. 8) to test a possible size reduction associated to their abundance decrease. Collected data show that the base width and the height fluctuate independently (R^2=0.31), but that the volume is highly correlated with the base width (R^2=0.81) and with a minor extent with the height (R^2=0.66). In Fig. 7, we illustrate the volume fluctuations as the three-point moving average of the volume curve. Average volume values of ca. 300 μm^3 measured in the interval preceding the Weissert-OAE and a moderate increase is observed at the onset of the OAE followed by a decrease (to ca. 250 μm^3) in correspondence of the climax of the $\delta^{13}C$ excursion. The interval following the Weissert-OAE is marked by a large increase in the average volume (to ca. 500 μm^3) during the recovery phase. The size variations of *N. steinmannii* do not show any correspondence with fluctuations in nannoconid total abundance indicating that these two parameters were independent and that the factor/s that caused the "nannoconid decline" did not affect the size of *N. steinmannii*.

The Italian pelagic record of the Weissert-OAE shows changes in nannofossil abundance and composition that have been overall documented in France (Duchamp et al 2014; Barbarin et al., 2012), in the Atlantic (Bornemann & Mutterlose, 2008) and in the Pacific (Erba et al., 2004) Oceans, thus demonstrating the supra-regional nature of the nannoplankton response. The Weissert-OAE differs from other Cretaceous OAEs since it was characterized by relatively cooler conditions, as for example documented by the occurrence of the nannofossil boreal species *Kokia borealis* at low latitudes in Romania (Melinte & Mutterlose, 2001) and Pacific Ocean (Erba et al., 2004). Therefore, the paleoenvironmental perturbations across the Weissert-OAE cannot be ascribed to global warming. The biocalcification crisis expressed by the "nannoconid decline" has been linked to

excess CO_2 and concurrent higher fertility (Bersezio et al., 2002; Erba & Tremolada, 2004; Erba et al., 2004; Weissert & Erba, 2004). Although ocean acidification as the triggering factor of the major decrease in abundance of the heavily calcified nannoconids has been disputed (Duchamp-Alphonse et al., 2007, 2014; Barbarin et al., 2012), there is a general consensus on the role of enhanced fertility (Bersezio et al., 2002; Erba et al., 2004; Duchamp-Alphonse et al., 2007, 2014; Bornemann & Mutterlose, 2008; Barbarin et al., 2012). The "nannoconid decline" is not paralleled by significant size variations of *N. steinmannii*, although larger specimens are observed in the recovery phase of the C isotopic curve at supraregional scale (Barbarin et al., 2012; this study)

The early Aptian OAE 1a

Nine Italian sections record the occurrence of OAE1a as traced by carbon isotope data (Fig. 9). In particular, the Pusiano, Piè del Dosso and Spiazzi sections in the Lombardy Basin, the Cismon Core and outcrop in the Belluno Basin, the Gorgo a Cerbara section and the Piobbico Core in the Umbria-Marche Basin, the Coppitella section in Gargano (Puglia, southern Italy) and the Calabianca section in Sicily. The Cismon APTICORE is the most studied record for OAE1a in Italy (Tab. 3). In fact, following the first work of Erba et al. (1999), a large amount of published literature has continuously extended and/or refined the C_{carb} and C_{org} chemostratigraphy, highlighting the importance of this core as a fundamental reference for the OAE1a interval. The distribution of the various sections allows for comparisons of the occurrence and extent of OAE1a in different basins. However, it must be noticed that not all the published records are complete, in particular the Spiazzi section lacks the vast majority of the event, preserving just the uppermost part of the carbon isotopic anomaly, while a hiatus removes the Ap3 and Ap 4 intervals of the carbon excursion in the Piobbico Core (Bottini et al., 2015).

Quantitative abundance data of nannofossil assemblages of the upper Barremian-lower Aptian are available for the Piè del Dosso, Cismon outcrop and Core, Gorgo a Cerbara, Piobbico Core, Coppitella and Calabianca (Erba, 1994; Bellanca et al., 2002; Erba & Tremolada, 2004; Bottini et al., 2015; Luciani et al., 2001). Slightly before the onset of OAE1a, the "nannoconid crisis" documents a major decrease of nannofossil calcite production, initiated close to the Barremian/Aptian boundary with the "nannoconid decline" associated with the appearance of small taxa that, together, seem to testify the response of calcareous nannoplankton to increased CO_2 and metal enrichment (Erba et al., 2015). The "nannoconid crisis" corresponds to a largest biocalcification failure, with a drop in pelagic biogenic calcite production of ~80% under excess CO_2, enhanced nutrient availability, global warming and possibly ocean acidification. The rock-forming nannoconids experienced a major, temporary failure during OAE1a but survived, presumably in sufficiently shielded ecological niches, to re-thrive when paleoenvironmental conditions ameliorated (Erba et al., 2015).

Morphometric data of *B. constans* obtained for the uppermost Barremian through Cenomanian interval of Italian sections (Erba et a., 2010; Faucher et al., 2017; this work) show that coccolith length and width are directly correlated (R^2=0.80) (Fig. 10), thus we only comment the fluctuations of the mean length, reported as the three-point moving average of the mean length curve. In the Cismon Core the coccolith length/width Pearson correlation is very high (R^2=0.90); *B. constans* shows a marked reduction in size in correspondence of the onset of the OAE 1a and minimum average size (ca. 3 μm) was reached in the core of the negative $\delta^{13}C$ segment Ap3 (Fig. 9). The mean *B. constans* length increases across segments Ap4 to Ap6 and remains relatively stable up to the end of OAE1a. A minor decrease in the average coccolith size is detected in segment Ap7.

Morphometric analyses of *N. steinmannii* performed in the Cismon Core (this study) highlight rather stable sizes through OAE1a. As for the Weissert-OAE, the base width and the height are not correlated but there is a correlation between the base width and the height with the volume (Fig. 8). The average volume is above 500 μm^3 prior to OAE1a and shows a minor decrease during the event. The only interval characterized by relatively smaller specimens (average volume comprised between 300 and 400 μm^3) coincides with the end of OAE1a (segments Ap6–base Ap7) (Fig. 9) that is followed by an interval of increased sizes during $\delta^{13}C$ segment Ap7 (Fig. 9). The average volume of *N. steinmannii* in the early Aptian (500 μm^3) is relatively higher compared to the Weissert-OAE (380 μm^3). But, similarly to the Valanginian Weissert-OAE, the *N. steinmanii* mean size does not show correlation with the nannoconid total abundance. In the specific case of OAE1a, the volume fluctuations of *N. steinmanii* do not follow size variations displayed by *B. constans* coccoliths.

The latest Barremian "nannoconid decline" and early Aptian "nannoconid crisis" have been documented at global scale (Erba, 1994, 2004; Erba et al., 2015) and are interpreted as the result of concurrent higher fertility and excess CO_2 that would have negatively affected the biocalcification process in calcareous nannoplankton (Erba & Tremolada, 2004; Erba et al., 2010, 2015). The coincidence of the "nannoconid decline" and "nannoconid crisis" with trace metal enrichments was further explained by hydrothermal activity releasing large quantities of biolimiting and/or toxic trace elements (Erba et al., 2015). The maximum perturbation was reached in the core of the negative $\delta^{13}C$ anomaly, when the highest temperatures, highest surface water fertility, the maximum ocean acidification and the maximum reduction of coccolith size occurred. The nannoconids responded to these perturbations with a severe reduction in the total abundance, but not significant size variations.

The latest Cenomanian OAE 2

Ten sections reporting the carbon isotope excursion for the OAE2 in Italy are described in the literature (Fig. 11). Most sections are Contessa sections and Gubbio S2 Core), but other outcrops document the OAE2 positive carbon isotopic excursion in the Belluno Basin (Cismon section) and

in Sicily (Novara di Sicilia, Calabianca and Guidaloca sections). Among all, the Bottaccione area represents a cornerstone for OAE2 C isotope chemostratigraphy in Italy (Tab. 4). In fact, following the seminal work of Scholle & Arthur (1980), many papers in the past 40 years have continuously documented the occurrence of the $\delta^{13}C$ positive anomaly characterizing OAE2 in the Gubbio succession. Even if the Umbria-Marche Basin remains a key-area for the stratigraphy of OAE2, recent advances in the carbon chemostratigraphy (Gambacorta et al., 2015, 2016), suggest that at Furlo, Contessa - Gubbio S2 Core, Monte Petrano and Gorgo a Cerbara sections a regional hiatus elides most of the C isotopic anomaly, namely the "plateau", the "c" peak and the first part of the recovery. Therefore, the OAE2 stratigraphic record in these sections was proved incomplete (Fig. 11). In Sicily, only the Calabianca section contains the entire $\delta^{13}C$ excursion, as the Novara di Sicilia and Guidaloca sections cover only the lower and uppermost part of the event, respectively.

Quantitative analyses of calcareous nannofloras are scanty for Italian sections, because the Bonarelli Level is barren of calcareous nannofossils, preventing the characterization of their modification during the paleoenvironmental perturbation. Changes in abundance across OAE2 were obtained for the Bottaccione section (Erba, 2004) and morphometric data were documented by Faucher et al. (2017) for the Novara di Sicilia section. In addition, quantitative nannofossil data are available for the intervals below and above the Bonarelli Level of the Furlo and Monte Petrano sections. The absence or extremely rareness of calcareous nannofossils across the OAE2 black shales of the Bonarelli Level is attributed to extreme acidification conditions (Erba, 2004). A drop in nannofossil abundance and species richness has been documented worldwide (Nederbragt & Fiorentino, 1999; Hardas & Mutterlose, 2007; Linnert et al., 2010, 2011; Corbett & Watkins, 2013) and interpreted as the result of eutrophic conditions perhaps combined with trace metal enrichments in surface water that could have favored phytoplanktonic group other than calcareous nannoplankton (Erba, 2004; Lignum et al., 2007; Linnert et al., 2010; Faucher et al., 2017). Indeed, *Biscutum* is interpreted as a higher fertility taxon but its drop in abundance might be evidence of trophic conditions above threshold values for calcareous nannoplankton during OAE 2 (Erba, 2004).

Morphometric data of *B. constans* across the latest Cenomanian OAE2 in the Novara di Sicilia section integrated with those gathered for the Eastbourne section (Faucher et al., 2017) are represented in Fig. 11. Coccoliths of *B. constans* show significant variations in size as traced by length and width. These two parameters are directly correlated (R^2=0.76) (Fig. 10), thus we only comment the fluctuations of the mean length, as smoothed in Fig. 11. At the OAE2 onset, *B. constans* shows a first decrease in size followed by an increase of coccolith size in $\delta^{13}C$ peak "a". A further size decrease culminates with dwarfism around $\delta^{13}C$ peak "b" where the smallest coccoliths are recorded (ca. 1.5 μm). Similar and coeval trends have been documented in a variety of settings as a biocalcification response to paleoenvironmental global stress. However, at Novara di Sicilia, *B. constans* coccoliths have the most reduced sizes compared to other sections: a

progressive decline in the average coccolith sizes goes hand in hand with the decrease in latitude (Faucher et al., 2017).

Calcareous nannofossil fluctuations in abundance and morphometry of selected taxa across the latest Cenomanian OAE2 are interpreted as caused by global warming, although interrupted by the cooling interlude of the Plenus Cold Event (Gale & Christensen, 1996; Gale et al., 2019), changes in ocean fertility and chemistry. The short return to larger *B. constans* coccoliths around $\delta^{13}C$ peak "a" occurs in the Plenus Cold Event: a cool-water preference was implied for *B. constans* (Lees et al., 2005) and may explain its increase in size during the cooling interval. The subsequent *B. constans* dwarfism correlates with the maximum ocean perturbation with metal enrichments, temperature rise and probably ocean acidification due to excess CO_2 (Erba, 2004; Snow et al., 2005; Jarvis et al., 2011; Du Vivier et al., 2015; Faucher et al., 2017). Only a partial return to pre-OAE2 sizes was observed in *B. constans* coccoliths after $\delta^{13}C$ peak "d" during the C isotopic recovery phase, suggesting the persistence of stressing conditions in the earliest Turonian.

CONCLUDING REMARKS

Our synthesis points out that Italian pelagic sections are key to quantify changes in calcareous nannoplankton during times of highly perturbed conditions associated with OAEs, as evidenced by $\delta^{13}C$ anomalies testifying discrete global alterations of the C cycle. Indeed, in addition to extreme climatic conditions and oceanic fertilization, OAEs were also times of altered chemistry making calcification difficult. It is possible that volcanically driven excess CO_2 in the ocean/atmosphere system (Jenkyns, 2010) induced ocean acidification (Erba et al., 2010) and caused crises of the dominant rock-forming calcareous nannoplankton forms. This seems the case for the "*Schizosphaerella* crisis", the "nannoconid decline" and the "nannoconid crisis" during the early Toarcian T-OAE, the late Valanginian Weissert-OAE and the early Aptian OAE1a, respectively. An even more dramatic drop in nannofossil abundance characterizes the latest Cenomanian OAE2, marked by a widespread biocalcification failure of calcareous nannoplankton taxa.

In addition to major changes in nannofossil abundance, a species-specific decrease in size has been detected for most OAEs, specifically for *Schizosphaerella* across the T-OAE and *B. constans* in the interval of maximum perturbation of both OAE1a and OAE2. Size of *N. steimannii*, instead, does not show significant variations across the Weissert-OAE and OAE1a. We underline that none of the taxa experiencing a calcification crisis and/or showing a size decrease got extinct: they recovered when the paleoenvironment returned to a pre-perturbation state, although the calcareous nannoplankton return to normal conditions occurred much slower than their response to environmental stress at the beginning of the OAE disturbance. After the T-OAE and OAE1a,

schizosphaerellids and nannoconids resumed in abundance, although nannofossil assemblages changed to a different composition. This was also due to originations of new species starting some 1 million years before the onset of the T-OAE and OAE1a and continuing through the events (Figs. 5 and 9), indicating that some calcareous nannoplankton taxa could innovate new forms of calcification, perhaps to overcome the stressing phase. These speciation episodes developed quickly, at an average rate of 1 first occurrence every 100-200k years, and in absence of extinctions suggesting resilience of this phytoplankton group.

The Italian pelagic record shows that the response of calcareous nannoplankton to paleoenvironmental perturbations of the Weissert-OAE and OAE2 was significantly different. The Valanginian "nannoconid decline" was gradual and less pronounced, as it was the recovery phase, while in the late Cenomanian the dramatic reduction in nannofossil total abundance is as sudden as the recovery after OAE2. As far as nannoplankton evolutionary patterns and rates are concerned, again the response to the Weissert-OAE and OAE2 was different relative to the T-OAE and OAE1a. During the late Valanginian-early Hauterivian (Fig. 7), a few first occurrences followed each other slowly, about one every 1 million years. Across OAE2, instead, extinctions occurred with a rate of one every 100-200k years at the onset or at the end of the event, while some originations are recorded from the middle part of OAE2 and continued afterwards (Fig. 11).

In conclusion, OAEs perturbations are fully recorded in pelagic micrites that trace shift in abundance of calcareous nannofossils and specifically of rock-forming taxa that at least partly and gradually resumed when paleoecosystem conditions ameliorated. Changes in biocalcification are further deduced by species-specific reduction in size under maximum stress during OEAs. The role of paleoenvironmental pressure on calcareous nannoplankton evolution during the early Toarcian T-OAE, late Valanginian Weissert-OAE, early Aptian OAE1a and latest Cenomanian OAE2, if any, was not univocal, but in general resulted in the origination of new taxa.

ACKNOWLEDGMENTS

We thank our Colleagues that contributed with thoughtful discussions to the comprehension of Jurassic and Cretaceous OAEs, particularly J.E.T. Channell, H. Jenkyns, I. Premoli Silva, and H. Weissert: with them we shared field work, especially in Italy, and scientific debates. M. Parente and I. Premoli Silva provided insightful reviews complementing the Editors' criticism. This synthesis benefitted, at various stages, of the financial support by MIUR-PRIN2011(2010X3PP8J) awarded to E.E. and SIR-2014 (MIUR–Scientific Independence of young Researchers) to C.B.

REFERENCES

Abramovich S., Keller G., Stüben D. & Berner Z. (2003). Characterization of late Campanian and Maastrichtian planktonic foraminiferal depth habitats and vital activities based on stable isotopes. *Palaeogeography Palaeoclimatology Palaeoecology*, 202: 1-29.

Arthur M. A. & Schlanger S. O. (1979). Cretaceous. AAPG bulletin, 63(6): 870-885.

Arthur M.A., Dean W.E. & Pratt. L.M. (1988). Geochemical and climatic effects of increased marine organic carbon burial at the Cenomanian/Turonian boundary. *Nature*, 335: 714-717.

Arthur M. A., Jenkyns H. C., Brumsack H.-J. & Schlanger S. O. (1990). Stratigraphy, geochemistry, and paleoceanography of organic-carbon-rich Cretaceous sequences, in Cretaceous Resources, Events and Rhythms, NATO ASI Ser., vol. 304, edited by R. N. Ginsburg and B. Beaudoin, pp. 75–119, Kluwer Acad., Dordrecht, Netherlands.

Barbarin N., Bonin A., Mattioli E., Pucéat E., Cappetta H., Gréselle B., Pittet B., Vennin E. & Joachimski M. (2012). Evidence for a complex Valanginian nannoconid decline in the Vocontian basin (South East France). *Marine Micropaleontology*, 84: 37-53.

Bellanca A., Erba E., Neri R., Premoli Silva I., Sprovieri M., Tremolada F. & Verga D. (2002). Paleoceanographic significance of the Tethyan ‘‘Livello Selli’’ (Early Aptian) from the Hybla Formation, northwestern Sicily: biostratigraphy and high-resolution chemostratigraphic records. *Palaeogeography, Palaeoclimatology, Palaeoecology*, 185: 175-196.

Bersezio R., Erba E., Gorza, M. & Riva, A. (2002). Berriasian–Aptian black shales of the Maiolica Formation (Lombardian Basin, Southern Alps, northern Italy): Local to global events: *Palaeogeography, Palaeoclimatology, Palaeoecology*, 180: 253–275, doi:10.1016/S0031-0182(01)00416-3.

Bornemann A., Mutterlose J. (2008). Calcareous nannofossil and $\delta^{13}C$ records from the Early Cretaceous of the Western Atlantic Ocean: evidence for enhanced fertilization across the Berriasian–Valanginian transition. *Palaios*, 23: 821–832.

Bottini C., & Erba E. (2018). Mid-Cretaceous paleoenvironmental changes in the western Tethys. *Climate of the Past*, 14(8): 1147-1163.

Bottini C., Erba E., Tiraboschi D., Jenkyns H. C., Schouten S. & Sinninghe Damsté J. S. (2015). Climate variability and ocean fertility during the Aptian Stage. *Climate of the Past,* 11: 383–402, https://doi.org/10.5194/cp-11-383-2015.

Bottini C., Dieni I., Erba E. & Massari F. (2018). The Valanginian Weissert Oceanic Anoxic Event Recorded in Central-Eastern Sardinia (Italy). *Rivista Italiana di Paleontologia e Stratigrafia*, 124(3): 617-637.

Bown P. R., Lees J. A. & Young J. R. (2004). Calcareous nannoplankton evolution and diversity through time. In *Coccolithophores* (pp. 481-508). Springer, Berlin, Heidelberg.

Breheret I. G. (1983). Sur des niveaux de black shales dans l'Albien inferieur et moyen du domaine vocontien (sud-est de la France): etude de nannofacies et signification des paleoenvironnements, *Bulletin du Muséum national d'histoire naturelle, Paris,* 5: 113-159.

Bucefalo Palliani R., Cirilli S. & Mattioli E. (1998). Phytoplankton response and geochemical evidence of the lower Toarcian relative sea level rise in the Umbria-Marche basin (Central Italy). *Palaeogeography, Palaeoclimatology, Palaeoecology*, 142: 33–50.

Casellato C. E. & Erba E. (2015). Calcareous nannofossil biostratigraphy and paleoceanography of the Toarcian Oceanic Anoxic Event at Colle di Sogno section (Southern Alps, Italy). *Rivista Italiana di Paleontologia e Stratigrafia*, 105: 343-376.

Channell J.E.T., Erba E. & Lini A. (1993). Magnetostratigraphic calibration of the Late Valanginian carbon isotope event in pelagic limestones from Northern Italy and Switzerland. *Earth Planetary Science Letters*, 118: 145-166.

Channell J.E.T., Erba E., Nakanishi M. & Tamaki K. (1995). Late Jurassic–Early Cretaceous time scales and oceanic magnetic anomaly block models, in Berggren, W.A., et al., eds., Geochronology, time scales and global stratigraphic correlation: SEPM (Society for Sedimentary Geology) Special Publication, 54: 51–63.

Claps M., Erba E., Masetti D. & Melchiorri F. (1995). Milankovitch-type cycles recorded in Toarcian black shales from the Belluno Trough (Southern Alps, Italy). *Memorie di Scienze Geologiche*, 47: 179-188.

Clémence M. E., Gardin S. & Bartolini A. (2015). New insights in the pattern and timing of the Early Jurassic calcareous nannofossil crisis. *Palaeogeography, Palaeoclimatology, Palaeoecology*, 427: 100-108.

Cobianchi M., Picotti V., (2001). Sedimentary and biological response to sea-level and palaeoceanographic changes of a Lower-Middle Jurassic Tethyan platform margin (Southern Alps, Italy). *Palaeogeography, Palaeoclimatology, Palaeoecology*, 169: 219–244.

Coccioni R., Nesci O., Tramontana M., Wezel F. C. & Moretti E. (1987). Descrizione di un livello-guida "radiolaritico-bituminoso-ittiolitico" alla base delle Marne a Fucoidi nell'Appennino Umbro-Marchigiano. *Bollettino della Società Geologica Italiana,* 106: 183,192.

Coccioni R., Erba E., Premoli Silva I., (1992). Barremian–Aptian calcareous plankton biostratigraphy from the Gorgo a Cerbara section (Marche, Central Italy) and implications for plankton evolution. *Cretaceous Research,* 13: 517– 537.

Corbett M. J. & Watkins D. K. (2013). Calcareous nannofossil paleoecology of the mid-Cretaceous Western Interior Seaway and evidence of oligotrophic surface waters during OAE2. *Palaeogeography, Palaeoclimatology, Palaeoecology*, 392: 510-523.

Corfield R.M., Cartlidge J.E., Premoli-Silva I. & Housley R.A. (1991). Oxygen and carbon isotope stratigraphy of the Palaeogene and Cretaceous limestones in the Bottaccione Gorge and the Contessa Highway sections, Umbria, Italy. *Terra Nova*, 3(4): 414-422.

Dal Piaz G. (1907). Le Alpi Feltrine. *Memorie del Reale Istituto Veneto di Scienze Lettere ed Arti*, 27/9: 176.

Dromart G., Garcia J.-P., Gaumet F., Picard S., Rousseau M., Atrops F., Lecuyer C. & Sheppard S.M.F. (2003). Perturbation of the carbon cycle at the Middle/Late Jurassic transition: geological and geochemical evidence. *Am. J. Sci.*, 303: 667-707.

Du Vivier A. D., Jacobson A. D., Lehn G. O., Selby,D., Hurtgen M. T. & Sageman B. B. (2015). Ca isotope stratigraphy across the Cenomanian–Turonian OAE 2: links between volcanism, seawater geochemistry, and the carbonate fractionation factor. *Earth and Planetary Science Letters,* 416: 121-131.

Duchamp-Alphonse S., Gardin S., Fiet N., Bartolini A., Blamart D. & Pagel M. (2007). Fertilization of the northwestern Tethys (Vocontian basin, SE France) during the Valanginian carbon isotope perturbation: evidence from calcareous nannofossils and trace element data. *Palaeogeography, Palaeoclimatology, Palaeoecology*, 243(1-2): 132-151.

Duchamp-Alphonse S., Gardin S., & Bartolini A. (2014). Calcareous nannofossil response to the Weissert episode (Early Cretaceous): Implications for palaeoecological and palaeoceanographic reconstructions. *Marine Micropaleontology*, 113: 65-78.

Erba E. (1994). Nannofossils and superplumes: the early Aptian nannoconid crisis. *Paleoceanography,* 9: 483– 501.

Erba E. (2004). Calcareous nannofossils and Mesozoic oceanic anoxic events. *Marine micropaleontology*, 52(1-4): 85-106.

Erba E. (2006). The first 150 million years history of calcareous nannoplankton: biosphere–geosphere interactions. *Palaeogeography, Palaeoclimatology, Palaeoecology*, 232(2-4): 237-250.

Erba E. & Tremolada F. (2004). Nannofossil carbonate fluxes during the Early Cretaceous: phytoplankton response to nutrification episodes, atmospheric CO_2 and anoxia. *Paleoceanography*, 19: 1–18, doi:10.1029/2003PA000884.

Erba E., Channell J.E.T., Claps M., Jones C., Larson R.L., Opdyke B., Premoli Silva I., Riva A., Salvini G. & Torricelli S. (1999). Integrated stratigraphy of the Cismon Apticore (Southern Alps, Italy): A “reference section” for the Barremian-Aptian interval at low latitudes. *Journal of Foraminiferal Research*, 29: 371-391.

Erba E., Bartolini A. & Larson R. L. (2004). Valanginian Weissert oceanic anoxic event. *Geology*, 32(2): 149-152.

Erba E., Bottini C., Weissert H. J. & Keller C. E. (2010). Calcareous nannoplankton response to surface-water acidification around Oceanic Anoxic Event 1a. *Science*, 329(5990): 428-432.

Erba E., Duncan R.A., Bottini C., Tiraboschi D., Weissert H., Jenkyns H.C. & Malinverno A. (2015). Environmental consequences of Ontong Java Plateau and Kerguelen Plateau volcanism. *Geological Society of America Special Paper*, 511: 271-303.

Erbacher J., Thurow J. & Littke R. (1996). Evolution patterns of radiolaria and organic matter variations: A new approach to identify sea-level changes in mid-Cretaceous pelagic environments. *Geology*, 24: 499-502.

Farinacci A. (1964). Microrganismi dei calcari 'Maiolica'e 'Scaglia'osservati al microscopio elettronico (nannoconi e coccolithophoridi). *Bollettino della Società Paleontologica Italiana*, 3(2): 172-181.

Faucher G., Erba E., Bottini C. & Gambacorta G. (2017). Calcareous nannoplankton response to the latest Cenomanian Oceanic Anoxic Event 2 perturbation. *Rivista Italiana di Paleontologia e Stratigrafia*, 123(1): 159-176.

Fraguas Á., Comas-Rengifo M. J., Gómez J. J. & Goy A. (2012). The calcareous nannofossil crisis in Northern Spain (Asturias province) linked to the Early Toarcian warming-driven mass extinction. *Marine Micropaleontology*, 94: 58-71.

Gaetani M., & Poliani G. (1978). I1 Toarciano ed il Giurassico medio in Albenza. *Rivista Italiana di Paleontologia e Stratigrafia,* 91: 295-320.

Gale A. S. & Christensen W. K. (1996). Occurrence of the belemnite Actinocamax plenus in the Cenomanian of SE France and its significance. *Bulletin of the Geological Society of Denmark*, 43(1): 68-77.

Gale A. S., Jenkyns H. C., Tsikos H., van Breugel Y., Sinninghe Damste J. S., Bottini C., Erba E., Russo F., Falzoni F., Petrizzo M.R., Dickson A.J. & Wray D.S. (2019). High-resolution bio- and chemostratigraphy of an expanded record of Oceanic Anoxic Event 2 (Late Cenomanian–Early Turonian) at Clot Chevalier, near Barrême, SE France (Vocontian Basin, SE France). *Newsletters on Stratigraphy*, 52/1: 97–129.

Gambacorta G., Jenkyns H.C., Russo F., Tsikos H., Wilson P.A., Faucher G. & Erba E. (2015). Carbon- and oxygen-isotope records of mid-Cretaceous Tethyan pelagic sequences from the Umbria–Marche and Belluno Basins (Italy). *Newsletters on Stratigraphy*, 48/3: 299-323.

Gambacorta G., Bersezio R., Weissert H. & Erba E. (2016). Onset and demise of Cretaceous oceanic anoxic events: The coupling of surface and bottom oceanic processes in two pelagic basins of the western Tethys. *Paleoceanography*, 31(6): 732-757.

Giorgioni M., Keller C. E., Weissert H., Hochuli P. A. & Bernasconi S. M. (2015). Black shales–from coolhouse to greenhouse (early Aptian). *Cretaceous Research*, 56: 716-731.

Gradstein F.M., Ogg J.G., Schmitz M.D. & Ogg G.M. (2012). The Geologic Time Scale 2012. *Amsterdam, Elsevier B.V*., 1176 p.

Gréselle B., Pittet B., Mattioli E., Joachimski M., Barbarin N., Riquier L., Reboulet S., Pucéat E. (2011). The Valanginian isotope event: a complex suite of palaeoenvironmental perturbations. *Palaeogeography, Palaeoclimatology, Palaeoecology,* 306: 41–57.

Hardas P. & Mutterlose J. (2007). Calcareous nannofossil assemblages of Oceanic Anoxic Event 2 in the equatorial Atlantic: Evidence of an eutrophication event. *Marine Micropaleontology*, 66(1): 52-69.

Hermoso M., Minoletti F., Rickaby R. E., Hesselbo S. P., Baudin F. & Jenkyns H. C. (2012). Dynamics of a stepped carbon-isotope excursion: Ultra high-resolution study of Early Toarcian environmental change. *Earth and Planetary Science Letters*, 319: 45-54.

Hesselbo S.P., Gröcke D., Jenkyns H.C., Bjerrum C.J., Farrimond P., Bell H.S.M. & Green O.R. (2000). Massive dissociation of gas hydrate during a Jurassic oceanic anoxic event. *Nature*, 406: 392-395.

Hesselbo S.P., Jenkyns H.C., Duarte L.V. & Oliveira L.C.V. (2007). Carbon-isotope record of the Early Jurassic (Toarcian) Oceanic Anoxic Event from fossil wood and marine carbonate (Lusitanian Basin, Portugal). *Earth and Planetary Science Letters*, 253: 455-470.

Jarvis I., Mabrouk A., Moody R.T.J. & Cabrera S.D. (2002). Late Cretaceous (Campanian) carbon isotope events, sea-level change and correlation of the Tethyan and Boreal realms. *Palaeogeography, Palaeoclimatology, Palaeoecology*, 188: 215-248.

Jarvis I., Gale A.S., Jenkyns H.C. & Pearce M.A. (2006). Secular variation in Late Cretaceous carbon isotopes: a new $\delta^{13}C$ carbonate reference curve for the Cenomanian–Campanian (99.6–70.6 Ma). *Geological Magazine,* 143: 561-608.

Jarvis, I., Lignum, J. S., Gröcke, D. R., Jenkyns, H. C., & Pearce, M. A. (2011). Black shale deposition, atmospheric CO2 drawdown, and cooling during the Cenomanian-Turonian Oceanic Anoxic Event. *Paleoceanography*, 26(3).

Jenkyns H.C. (1980). Cretaceous anoxic events: From continents to oceans. *Journal of the Geological Society of London,* 137: 171-188.

Jenkyns H. C. (1985). The Early Toarcian and Cenomanian–Turonian anoxic events in Europe: Comparisons and contrasts. *Geol. Rundsch.,* 74: 505–518, doi:10.1007/BF01821208.

Jenkyns H.C. (1988). The Early Toarcian (Jurassic) anoxic event: stratigraphic, sedimentary, and geochemical evidence. *The American Journal of Science* 288: 101–151.

Jenkyns H. C. (2010). Geochemistry of oceanic anoxic events. *Geochemistry, Geophysics, Geosystems,* 11(3).

Jenkyns H.C. & Clayton C.C. (1986). Black shales and carbon isotopes in pelagic sediments from the Tethyan Lower Jurassic. *Sedimentology*, 33: 87-106.

Jenkyns H.C., Gale A.S. & Corfield R.M. (1994). Carbon- and oxygen-isotope stratigraphy of the English Chalk and Italian Scaglia and its palaeoclimatic significance. *Geological Magazine*, 131: 1-34.

Jenkyns H.C., Gröcke D.R. & Hesselbo S.P. (2001). Nitrogen isotope evidence for water mass denitrification during the early Toarcian (Jurassic) oceanic anoxic event. *Paleoceanography*, 16 (6): 593-603.

Jenkyns H.C., Matthews A., Tsikos H. & Erel Y. (2007). Nitrate reduction, sulfate reduction, and sedimentary iron isotope evolution during the Cenomanian-Turonian oceanic anoxic event. *Paleoceanography*, 22, PA3208, doi:10.1029/2006PA001355.

Jenkyns H. C., Dickson A. J., Ruhl M., & Van den Boorn S. H. (2017). Basalt-seawater interaction, the Plenus Cold Event, enhanced weathering and geochemical change: deconstructing Oceanic Anoxic Event 2 (Cenomanian–Turonian, Late Cretaceous). *Sedimentology*, 64(1): 16-43.

Kàlin O. & Bernoulli D. (1984). Schizosphaerella Deflandre and Dangeard in Jurassic deeper-water carbonate sediments, Mazagan Continental Margin (Hole 547b) and Mesozoic Tethys In: Hinz, K., Winterer, E. L., et al., *Initial Reports DSDP* 79: Washington (U.S. Govt. Printing Office).

Keller C.E., Hochuli P.A., Weissert H., Bernasconi S.M., Giorgioni M. & Garcia T.I. (2011). A volcanically induced climate warming and floral change preceded the onset of OAE1a (Early Cretaceous). *Palaeogeography, Palaeoclimatology, Palaeoecology*, 305: 43-49.

Kuroda J., Ogawa N.O., Tanimizu M., Coffin M., Tokuyama H., Kitazato H. & Ohkouchi N. (2007). Contemporaneous massive subaerial volcanism and late Cretaceous Oceanic Anoxic Event 2. *Earth and Planetary Science Letters*, 256: 211-223.

Leckie R. M., Bralower T. J. & Cashman R. (2002). Oceanic anoxic events and plankton evolution: Biotic response to tectonic forcing during the mid-Cretaceous. *Paleoceanography*, 17(3): 13-1.

Lees J. A., Bown P. R., & Mattioli E. (2005). Problems with proxies? Cautionary tales of calcareous nannofossil paleoenvironmental indicators. *Micropaleontology*, 51(4): 333-343.

Lignum J., Jarvis I. & Pearce M. (2007). The dinoflagellate cyst record of the Cenomanian–Turonian boundary (OAE 2): Data from a newly cored black shale succession, Wunstorf, northern Germany. In *Geophysical Research Abstracts,* 9: 3854.

Lini A., Weissert H. & Erba E. (1992). The Valanginian carbon isotope event: a first episode of greenhouse climate conditions during the Cretaceous. *Global Change Special Issue, Terra Nova*: 4: 374-384.

Linnert C., Mutterlose J. & Erbacher J. (2010). Calcareous nannofossils of the Cenomanian/Turonian boundary interval from the Boreal Realm (Wunstorf, northwest Germany). *Marine Micropaleontology*, 74(1-2): 38-58.

Linnert C., Mutterlose J., & Mortimore R. (2011). Calcareous nannofossils from Eastbourne (southeastern England) and the paleoceanography of the Cenomanian–Turonian boundary interval. *Palaios*, 26(5): 298-313.

Lohmann H. (1902). Die Coccolithophoridae, eine Monographie der Coccolithen bildenden Flagellaten, zugleich ein Beitrat zur Kenntnis des Mittelmeerauftriebs. *Arch. Protistenkd*., 1: 89– 165.

Luciani V., Cobianchi M. & Jenkyns H.C. (2001). Biotic and geochemical response to anoxic events: the Aptian pelagic succession of the Gargano Promontory (southern Italy). *Geological Magazine*, 138: 277-298.

Malinverno A., Erba E. & Herbert T.D. (2010). Orbital tuning as an inverse problem: Chronology of the early Aptian oceanic anoxic event 1a (Selli Level) in the Cismon APTICORE: *Paleoceanography*, 25: PA2203, doi:10.1029/2009PA001769.

Malinverno A., Hildebrandt J., Tominaga M. & Channell J.E.T. (2012). M-sequence geomagnetic polarity time scale (MHTC12) that steadies global spreading rates and incorporates astrochronology constraints. *Journal of Geophysical Research*, 117: B06104, doi:10.1029/2012JB009260

Mattioli E. (1997). Nannoplankton productivity and diagenesis in the rhythmically bedded Toarcian-Aalenian Fiuminata section (Umbria-Marche Apennine, central Italy). *Palaeogeography, Palaeoclimatology, Palaeoecology,* 130 (1–4): 113-133.

Mattioli E. & Pittet B. (2002). The contribution of calcareous nannoplankton to the carbonate production in the Early Jurassic. *Marine Micropaleontol*ogy, 45: 175–190.

Mattioli E. & Pittet B. (2004). Spatial and temporal distribution of calcareous nannofossils along a proximal-distal transect in the Umbria-Marche basin (Lower Jurassic; Italy*). Palaeogeography, Palaeoclimatology, Palaeoecology*, 205: 295–316, doi:10.1016/j.palaeo.2003.12.013.

Mattioli E., Pittet B., Young J. R. & Bown P. R. (2004a). Biometric analysis of Pliensbachian-Toarcian (Lower Jurassic) coccoliths of the family Biscutaceae: Intra- and interspecific variability versus palaeoenvironmental influence, *Marine Micropaleontology,* 52: 5–27, doi:10.1016/j.marmicro.2004.04.004.

Mattioli E., Pittet B., Bucefalo Palliani R., Röhl H. J., Schmid-Röhl A. & Morettini E. (2004b). Phytoplankton evidence for the timing and correlation of palaeoceanographical changes during the early Toarcian oceanic anoxic event (Early Jurassic). *Journal of the Geological Society of London*, 161: 685 – 693, doi:10.1144/0016-764903-074.

Mattioli E., Pittet B., Suan G. & Mailliot S. (2008). Calcareous nannoplankton changes across the early Toarcian oceanic anoxic event in the western Tethys. *Paleoceanography and Paleoclimatology,* 23(3).

Mattioli E., Pittet B., Petitpierre L., Mailliot S., (2009). Dramatic decrease of pelagic carbonate production by nannoplankton across the early Toarcian anoxic event (T-OAE). *Global Planetary Chang*e, 65: 134–145.

Mattioli E., Pittet B., Riquier L. & Grossi V. (2014). The mid-Valanginian Weissert Event as recorded by calcareous nannoplankton in the Vocontian Basin. *Palaeogeography, Palaeoclimatology, Palaeoecology*, 414: 472-485.

Méhay S., Keller C.E., Bernasconi S.M., Weissert H., Erba E., Bottini C. & Hochuli P.A. (2009). A volcanic CO_2 pulse triggered the Cretaceous Oceanic Anoxic Event 1a and a biocalcification crisis: *Geology*, 37: 819–822, doi:10.1130/G30100A.1.

Melinte M. & Mutterlose J. (2001). A Valanginian (Early Cretaceous) 'boreal nannoplankton excursion' in sections from Romania. *Marine Micropaleontology*, 43: 1–25.

Menegatti A.P., Weissert H., Brown R.S., Tyson R.V., Farrimond P., Strasser A. & Caron M. (1998). High resolution $\delta^{13}C$ stratigraphy through the early Aptian "Livello Selli" of the Alpine Tethys. *Paleoceanography*, 13: 530-545.

Morettini E., Santantonio M., Bartolini A., Cecca F., Baumgartner P.O. & Hunziker, J.C. (2002). Carbon isotope stratigraphy and carbonate production during the Early-Middle Jurassic: examples from the Umbria-Marche- Sabina Apennines (central Italy). *Palaeogeography, Palaeoclimatology, Palaeoecology*, 184: 251-273.

Mort H., Jacquat O., Adatte T., Steinmann P., Fölmi K., Matera V., Berner Z. & Stüben D. (2007). The Cenomanian/Turonian anoxic event at the Bonarelli level in Italy and Spain: enhanced productivity and/or better preservation? *Cretaceous Research*, 28: 597-612.

Nederbragt A. J. & Fiorentino A. (1999). Stratigraphy and palaeoceanography of the Cenomanian-Turonian boundary event in Oued Mellegue, north-western Tunisia. *Cretaceous Research*, 20(1): 47-62.

Noël D., & Busson G. (1990). L'importance des schizosphères, stomiosphères, Conusphaera et Nannoconus dans la genèse des calcaires fins pélagiques du Jurassique et du Crétacé inférieur/Importance of schizospheres, stomiospheres, Conusphaera and Nannoconus in the genesis of Jurassic and Early Cretaceous fine-grained pelagic limestones. Sciences *Géologiques, bulletins et mémoires*, 43(1): 63-93.

Peti L., Thibault N., Clémence M. E., Korte C., Dommergues J. L., Bougeault C., Pellenard P., Jelby M.E. & Ullmann C. V. (2017). Sinemurian–Pliensbachian calcareous nannofossil biostratigraphy and organic carbon isotope stratigraphy in the Paris Basin: Calibration to the ammonite biozonation of NW Europe. *Palaeogeography, Palaeoclimatology, Palaeoecology*, 468: 142-161.

Premoli Silva, I., Erba, E., & Tornaghi, M.E. (1989). Paleoenvironmental signals and changes in surface fertility in mid Cretaceous Corg–rich pelagic facies of the Fucoid Marls (central Italy). *Geobios*, 22: 225–236, doi:10.1016/S0016-6995(89)80059-2.

Premoli Silva I., Erba E., Salvini G., Verga D. & Locatelli C. (1999). Biotic changes in Cretaceous anoxic events. *Journal of Foraminiferal Research*, 29: 352–370.

Renard M. (1986). Pelagic carbonate chemostratigraphy (Sr, Mg, ^{18}O, ^{13}C). Marine *Micropaleontology*, 10: 117-164.

Robinson S.A., Heimhofer U., Hesselbo S.P. & Petrizzo M.R. (2017). Mesozoic climates and oceans – a tribute to Hugh Jenkyns and Helmut Weissert. *Sedimentology*, 64: 1-15.

Sabatino N., Neri R., Bellanca A., Jenkyns H.C., Baudin F., Parisi G. & Masetti D. (2009). Carbon-isotope records of the Early Jurassic (Toarcian) oceanic anoxic event from the Valdorbia (Umbria–Marche Apennines) and Monte Mangart (Julian Alps) sections: palaeoceanographic and stratigraphic implications. *Sedimentology*, 56: 1307-1328.

Schindelin J., Arganda-Carreras I., Frise E., Kaynig V., Longair M., Pietzsch T., ... & Tinevez, J. Y. (2012). Fiji: an open-source platform for biological-image analysis. *Nature methods*, 9(7): 676. doi:10.1038/nmeth.2019

Schlanger S.O. & Jenkyns H.C. (1976). Cretaceous oceanic anoxic events: Causes and consequences. *Geologie en Mijnbouw*, 55: 179-184.

Scholle P.A. & Arthur M.A. (1980). Carbon isotope fluctuations in Cretaceous pelagic limestones: potential stratigraphic and petroleum exploration tool. *The American Association of Petroleum Geologists Bulletin*, 64 (1): 67-87.

Scopelliti G., Bellanca A., Coccioni R., Luciani V., Neri R., Baudin F., Chiari M. & Marcucci M. (2004). High-resolution geochemical and biotic records of the Tethyan 'Bonarelli Level' (OAE2, latest Cenomanian) from the Calabianca–Guidaloca composite section, northwestern Sicily, Italy. *Palaeogeography, Palaeoclimatology, Palaeoecology*, 208: 293-317.

Scopelliti G., Bellanca A., Erba E., Jenkyns H.C., Neri R., Tamagnini P., Luciani V. & Masetti, D. (2008). Cenomanian–Turonian carbonate and organic-carbon isotope records, biostratigraphy and provenance of a key section in NE Sicily, Italy: Palaeoceanographic and palaeogeographic implications. *Palaeogeography, Palaeoclimatology, Palaeoecology*, 265(1-2): 59–77.

Scotese C.R. ed. (2014). Atlas of Plate Tectonic Reconstructions (Mollweide Projection), Volumes 1-6, *PALEOMAP Project PaleoAtlas for ArcGIS*, PALEOMAP Project, Evanston, IL.

Snow L. J., Duncan R. A., & Bralower T. J. (2005). Trace element abundances in the Rock Canyon Anticline, Pueblo, Colorado, marine sedimentary section and their relationship to Caribbean plateau construction and oxygen anoxic event 2. *Paleoceanography and Paleoclimatology*, 20(3).

Sprovieri M., Coccioni R., Lirer F., Pelosi N. & Lozar F. (2006). Orbital tuning of a lower Cretaceous composite record (Maiolica Formation, central Italy). *Paleoceanography*, 21: PA4212, doi:10.1029/2005PA001224.

Sprovieri M., Sabatino N., Pelosi N., Batenburg S.J., Coccioni R., Iavarone M. & Mazzola S. (2013). Late Cretaceous orbitally-paced carbon isotope stratigraphy from the Bottaccione Gorge (Italy). *Palaeogeography, Palaeoclimatology, Palaeoecology*, 379-380: 81-94.

Stein M., Föllmi K.B., Westermann S., Godet A., Adatte T., Matera V., Fleitmann D., Berner Z. (2011). Progressive palaeoenvironmental change during the Late Barremian–Early Aptian as prelude to Oceanic Anoxic Event 1a: Evidence from the Gorgo a Cerbara section (Umbria-Marche basin, central Italy). *Palaeogeography, Palaeoclimatology, Palaeoecology*, 302: 396-406.

Stoll H.M. & Schrag D.P. (2000). High-resolution stable isotope records from the Upper Cretaceous rocks of Italy and Spain: glacial episodes in a greenhouse planet? *Geological Society of America Bulletin*, 112: 308–319.

Suan G., Mattioli E., Pittet B., Mailliot S., Lécuyer C. (2008). Evidence for major environmental perturbation prior to and during the Toarcian (Early Jurassic) oceanic anoxic event from the Lusitanian Basin, Portugal. *Paleoceanography* 23.

Suan G., Mattioli E., Pittet B., Lecuyer C., Sucheras-Marx B., Duarte L.V., Philippe M., Reggiani L., Martineau F. (2010). Secular environmental precursors to Early Toarcian (Jurassic) extreme climate changes. *Earth and Planetary Science Letters,* 290: 448–458.

Tejada M.L.G., Katsuhiko S., Kuroda J., Coccioni R., Mahoney J.J., Ohkouchi N., Sakamoto T. & Tatsumi Y. (2009). Ontong Java Plateau eruption as a trigger for the early Aptian oceanic anoxic event. *Geology*, 37: 855-858.

Tremolada F. & Erba E. (2002). Morphometric analysis of the Aptian *Rucinolithus terebrodentarius* and *Assipetra infracretacea* nannoliths: Implications for taxonomy, biostratigraphy and Paleoceanography. *Marine Micropaleontology*, 44: 77–92, doi:10.1016/S0377-8398(01)00038-X.

Tremolada F., Van de Schootbrugge B. & Erba E. (2005). Early Jurassic schizosphaerellid crisis in Cantabria, Spain: implications for calcification rates and phytoplankton evolution across the Toarcian oceanic anoxic event. *Paleoceanography*, 20(2).

Tiraboschi D., Erba E., & Jenkyns H. C. (2009). Origin of rhythmic Albian black shales (Piobbico core, central Italy): Calcareous nannofossil quantitative and statistical analyses and paleoceanographic reconstructions. *Paleoceanography and Paleoclimatology*, 24(2).

Tsikos H., Jenkyns H. C., Walsworth-Bell B., Petrizzo M. R., Forster A., Kolonic S., Erba E., Premoli Silva I., Baas M., Wagner T. & Sinninghe Damsté J.S. (2004). Carbon-isotope stratigraphy recorded by the Cenomanian–Turonian Oceanic Anoxic Event: correlation and

implications based on three key localities. *Journal of the Geological Society*, London, 161: 711-719.

van Breugel Y., Schouten S., Tsikos H., Erba E., Price G.D., & Sinninghe Damsté J.S. (2007). Synchronous negative carbon isotope shifts in marine and terrestrial biomarkers at the onset of the early Aptian oceanic anoxic event 1a: Evidence for the release of 13C-depleted carbon into the atmosphere. *Paleoceanography*, v. 22, PA1210, doi:10.1029/2006PA001341.

Van de Schootbrugge B., Bailey T.R., Rosenthal Y., Katz M.E., Wright J.D., Miller K.G., Feist-Burkhardt S. & Falkowski P.G. (2005) Early Jurassic climate change and the radiation of organic-walled phytoplankton in the Tethys Ocean. *Paleobiology*, 31: 73-97.

Voigt S., Aurag A., Leis F., Kaplan U., 2007. Late Cenomanian to Middle Turonian high-resolution carbon isotope stratigraphy: New data from the Münsterland Cretaceous Basin, Germany. *Earth and Planetary Science Letters*, 253: 196-210.

Weissert H. (1989). C-isotope stratigraphy, a monitor of paleoenvironmental change: a case study from the Early Cretaceous. *Surveys in Geophysics*, 10(1): 1-61.

Weissert H., Erba E. (2004). Volcanism, CO_2 and palaeoclimate: a Late Jurassic–Early Cretaceous carbon and oxygen isotope record. *Journal of the Geological Society*, 161: 695–702.

Weissert H., McKenzie J.A. & Channell J.E.T. (1985). Natural variations in the carbon cycle during the Early Cretaceous. *In* Sundquist, E.T., Broecker, W.S. (eds), The Carbon Cycle and Atmospheric CO_2: Natural variations Archean to the Present. *Geophysical Monography*, 32: 531-545.

Weissert H., Lini A., Föllmi K.B. & Kuhn O. (1998). Correlation of Early Cretaceous carbon isotope stratigraphy and platform drowning events: a possible link?. *Palaeogeography, Palaeoclimatology, Palaeoecology,* 137: 189-203.

CAPTIONS

Fig. 1 – A) Livello a Pesci, deposited during the T-OAE, at the Colle di Sogno section (n. 3 in Fig. 3 - Lombardy Basin, northwestern Italy); B) Livello a Pesci in the Sogno Core compared to the equivalent outcropping litostratigraphic interval (n. 3 in Fig. 3 - Lombardy Basin, northwestern Italy); C) Selli Level, deposited during the OAE1a, at the Apecchiese section. The laterally equivalent interval was cored nearby in the Piobbico Core (n. 17 in Fig. 3 - Umbria-Marche Basin, central Italy); D) Selli Level equivalent recovered with the Cismon APTICORE placed next to the same outcropping litostratigraphic interval (n. 11 and 12 in Fig. 3 - Belluno Basin, northeastern Italy); E) The Weissert-OAE interval (bounded by the two yellow dashed lines) at Polaveno (n. 6 in Fig. 3 - Lombardy Basin, northwestern Italy); F) The middle Cenomanian to lower Turonian succession at Furlo (n. 15 in Fig. 3 - Umbria-Marche Basin, central Italy) with the black shales of the Livello Bonarelli deposited during OAE2; G) Close up view of Livello Bonarelli in the Contessa outcrop (n. 24 in Fig. 3 - Umbria-Marche Basin, central Italy); H) Close up view of Livello Bonarelli in the Bottaccione Gorge section (n. 22 in Fig. 3 - Umbria-Marche Basin, central Italy); I) Close up view of Livello Bonarelli in the Monte Petrano section (n. 18 in Fig. 3 - Umbria-Marche Basin, central Italy).

Fig. 2 - Bulk carbonate carbon isotope ($\delta^{13}C_{carb}$) stratigraphy of the Jurassic and Cretaceous (modified after Robinson et al., 2017). The stratigraphic position of T-OAE, Weissert-OAE, OAE1a and OAE2 are reported as grey bands. Carbon-isotope data from: (1) Van de Schootbrugge et al. (2005); (2) Hesselbo et al. (2000); (3) Morettini et al. (2002); (4) Dromart et al. (2003); (5) Weissert et al. (1998); (6) Erbacher et al. (1996); (7) Jenkyns et al. (1994); (8) Jarvis et al. (2002); and (9) Abramovich et al. (2003). On the right the relative position of Italy at 180 Ma, 135 Ma, 120 Ma and 95 Ma is reported as a red outline on paleogeographic maps (modified after Scotese, 2014).

Fig. 3- Geographic location of the Italian sections with available quantitative and morphometric nannofossil and/or carbon isotope data for the T-OAE, Weissert-OAE, OAE1a and OAE2.

Fig. 4 – Measured parameters of selected nannofossil taxa: A) *N. steinmannii*; B) *B. constans* and C) *Schizosphaerella*.

Fig. 5 – On the left: synthesis of calcareous nannofossil changes through the Toarcian-OAE (ca. 183 Ma). Nannofossil origination and extinction intervals are reported as pink and blue bars, respectively. The *Schizosphaerella* and *M. jansae* variations in abundance and the diameter of

Schizospharella (three point moving average of the diameter) are reported (this study). On the right: the stratigraphic extent of published (semi)quantitative nannofossil data (red bar) and available inorganic and/or organic stable carbon isotope record (black bar) is reported for each section. Section numbering as in Fig. 3. The T-OAE is indicated with a grey band. The time scale is after Gradstein et al. (2012). Carbon isotope curve is modified after Hesselbo et al. (2007), Peniche section (Portugal).

Fig. 6 – A, B, C, D) Images of *Schizosphaerella* from the Colle di Sogno section (after Casellato & Erba, 2015); scale bar = 2 □m. A) Scanning electron microscope of a schizosphaerella-micrite from the uppermost Domaro Limestone. B) Light polarizing microscope image of a cluster of *Schizosphaerella* from the uppermost Domaro Limestone. C) Light polarizing microscope image of *S. punctulata* from the topmost Domaro Limestone. D) Light polarizing microscope image of "small *S. punctulata*" from the lowermost Sogno Formation. E, F, G) Results of mixture analysis of samples with estimated mean diameter (M), median diameter (MD) and number of specimens analyzed (N) subdivided in three intervals: E) pre- T-OAE, F) T-OAE and G) post T-OAE, analysed in the Colle di Sogno section and Sogno Core (this study).

Fig. 7 - On the left: synthesis of calcareous nannofossil changes through the Weissert-OAE (ca. 134 Ma). Nannofossil origination and extinction intervals are reported as pink and blue bars, respectively. The nannoconid variations in abundance (Erba & Tremolada, 2004) and the volume of *N. steinmannii* (three point moving average of the volume, this study) are reported. The extent of the *Diazomatolithus* acme, the *pentalith* abundance peak and the presence of *K. borealis* are also represented (Bersezio et al., 2002; Erba & Tremolada, 2004). On the right: the stratigraphic extent of published (semi)quantitative nannofossil data (red bar) and available inorganic and/or organic stable carbon isotope record (black bar) is reported for each section. Section numbering as in Fig. 3. The Weissert-OAE is indicated with a grey band. The time scale is from Channell et al. (1995). Carbon isotope curve is modified after Channell et al. (1993) (Capriolo section).

Fig. 8 – A) Scanning electron microscope image of a nannoconid-micrite from the Maiolica limestone of the Gorgo a Cerbara section. Nannoconids are marked by "N", on the left side, indicated by the arrow, there is a coccosphere of *Watznaueria barnesiae* (after Erba, 1994). B) Scatter plots of *N. steinmannii* base width, height and volume with Pearson correlation coefficient (r) and the number of measurements (N). Blue circles refer to the Polaveno section (Valanginian Weissert-OAE), orange circles refer to the Cismon Core (early Aptian OAE1a).

Fig. 9 - On the left: synthesis of calcareous nannofossil changes through the early Aptian OAE1a (ca. 120 Ma). Nannofossil origination intervals are reported as pink bars. The nannoconid variations in abundance (Erba & Tremolada, 2004; Bottini et al., 2015), the volume of *N. steinmannii* (three point moving average of the volume, this study) and the length of *B. constans* (three point moving average of the length, Erba et al., 2010) are reported. The pentalith abundance peak is also represented (Erba & Tremolada, 2004). Nannofossil-based temperature and nutrient indices are after Bottini et al. (2015). On the right: the stratigraphic extent of published (semi)quantitative nannofossil data (red bar) and available inorganic and/or organic stable carbon isotope record (black bar) is reported for each section. The occurrence of a hiatus is indicated with a dashed line. Section numbering as in Fig. 3. The OAE1a is indicated with a grey band. The time scale is from Malinverno et al. (2010, 2012). Carbon isotope curve is modified after Bottini et al. (2015), Cismon Core (Italy). Identification of segments of the carbon isotopic anomaly across OAE 1a follows Bottini et al. (2015).

Fig. 10 - Scatter plots of *B. constans* length and width with Pearson correlation coefficient (r) and the number of measurements (N). A) scatter plot of *B. constans* length and width measured in uppermost Barremian-Cenomanian Italian sections (Erba et al., 2010; Faucher et al., 2017; this work). B) scatter plots of *B. constans* length and width measured across the early Aptian-OAE1a in the Cismon Core (Erba et al., 2010); C) Scatter plots of *B. constans* across the Cenomanian/Turonian OAE2 from Novara di Sicilia section (Faucher et al., 2017).

Fig. 11 - On the left: synthesis of calcareous nannofossil changes through the Cenomanian/Turonian OAE2 (ca. 94 Ma). Nannofossil origination and extinction intervals are reported as pink and blue bars, respectively. The total nannofossil abundance variations (from Gubbio section, Erba, 1994) and the length of *B. constans* (three point moving average of the mean length, Faucher et al., 2017) are reported. Nannofossil based-nutrient index and *E. floralis* peaks are from Erba (2004). Cooling intervals are from (Jenkyns et al., 2017). On the right: the stratigraphic extent of published (semi)quantitative nannofossil data (red bar) and available inorganic and/or organic stable carbon isotope record (black bar) is reported for each section. The occurrence of a hiatus is indicated with a dashed line. Considering the proximity of the sites, we assume an extent of the hiatus for the Contessa and Bottaccione Gorge sections equal to that observed on the Gubbio S2 Core. Section numbering as in Fig. 3. The OAE2 is indicated with a grey band. The time scale is modified after Gradstein et al. (2012). Carbon isotope curve is modified after Tsikos et al. (2004), Eastbourne section (UK). Identification of individual peaks of the carbon isotopic anomaly across OAE2 follows Voigt et al. (2007).

Tab. 1 – Compilation of papers documenting quantitative nannofossil and carbon isotope data for the T-OAE interval

Tab. 2 – Compilation of papers documenting quantitative nannofossil and carbon isotope data for the Weissert-OAE interval

Tab. 3 – Compilation of papers documenting quantitative nannofossil and carbon isotope data for the OAE1a interval

Tab. 4 – Compilation of papers documenting quantitative nannofossil and carbon isotope data for the OAE2 interval

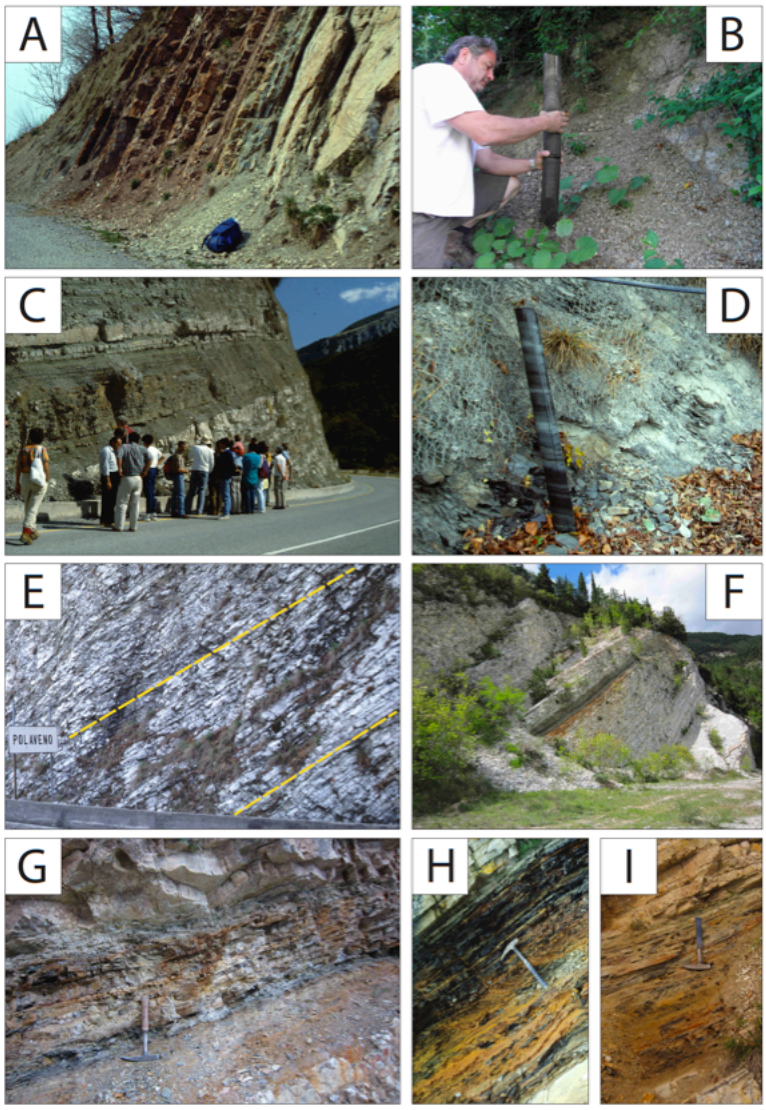

Fig.1

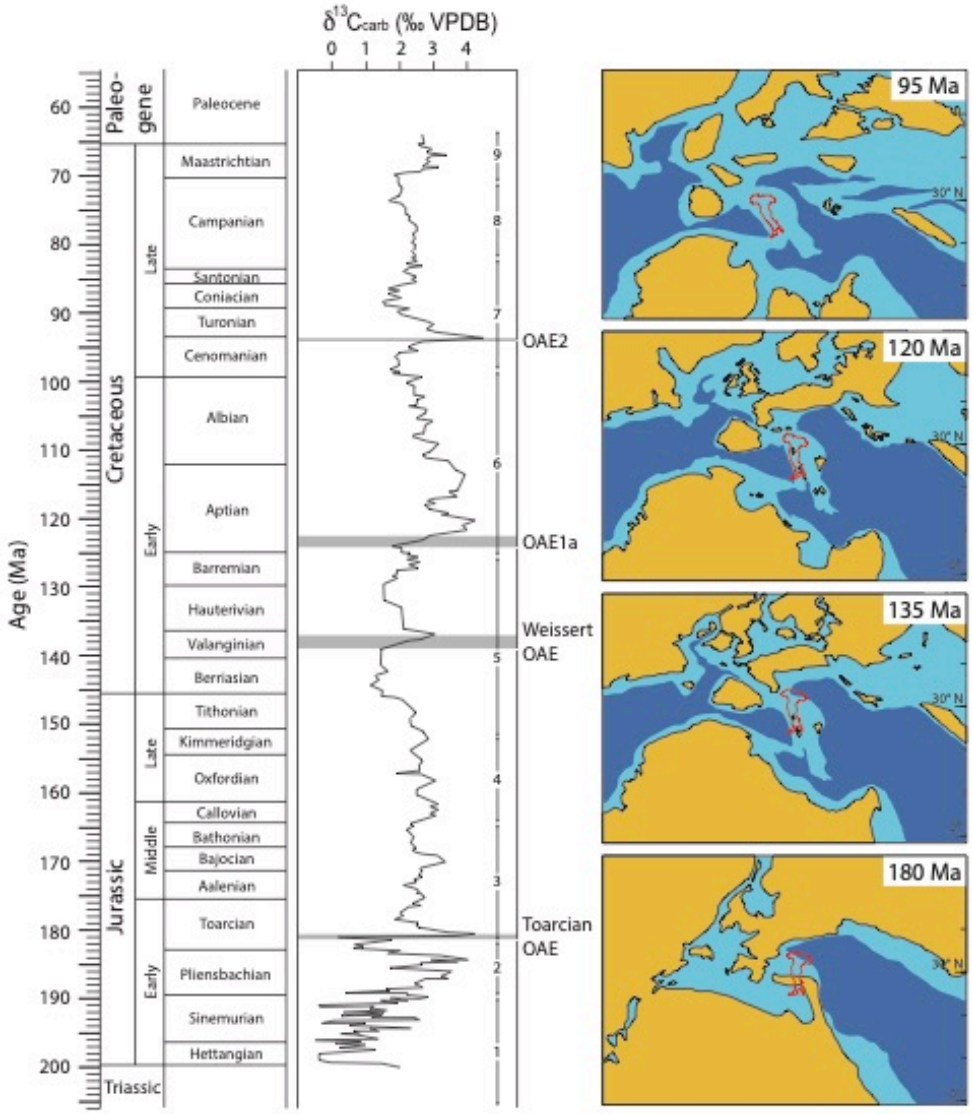
δ13Ccarb (‰ VPDB)
0 1 2 3 4
Age (Ma)
Paleo-gene
Cretaceous
Jurassic
Triassic
Late
Early
Middle
Paleocene
Maastrichtian
Campanian
Santonian
Coniacian
Turonian
Cenomanian
Albian
Aptian
Barremian
Hauterivian
Valanginian
Berriasian
Tithonian
Kimmeridgian
Oxfordian
Callovian
Bathonian
Bajocian
Aalenian
Toarcian
Pliensbachian
Sinemurian
Hettangian
OAE2
OAE1a
Weissert OAE
Toarcian OAE
95 Ma
120 Ma
135 Ma
180 Ma
30° N

Fig. 2

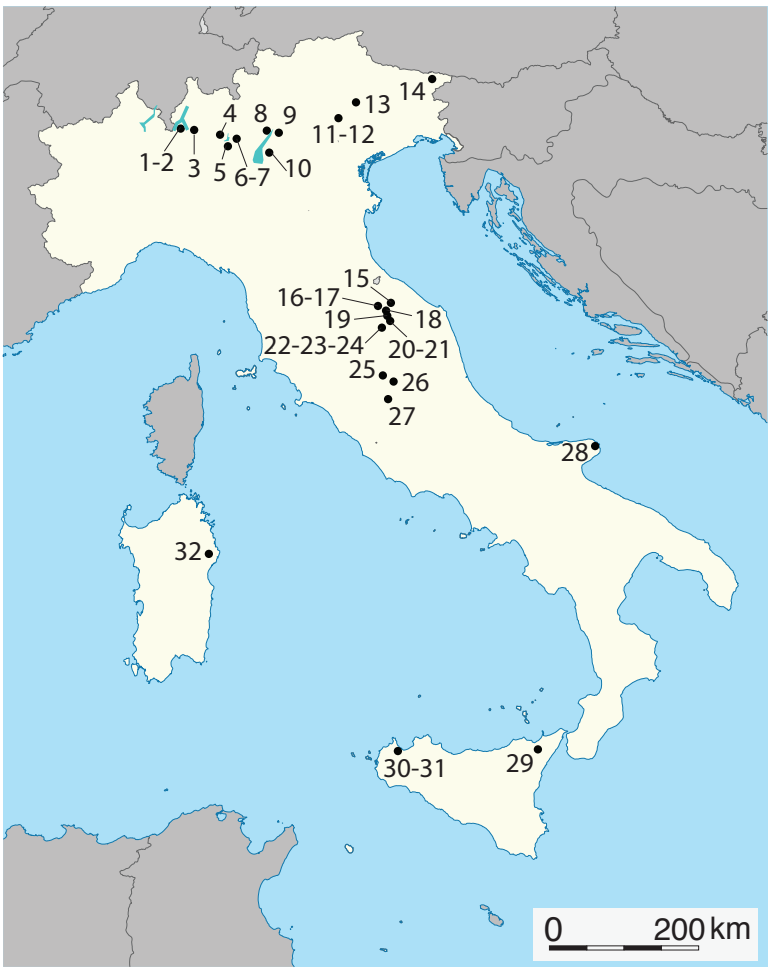

1 - Val Ceppelline (T-OAE)
2 - Pusiano (Weissert-OAE, OAE1a)
3 - Colle di Sogno (T-OAE)
4 - Rio-Corna (Weissert-OAE)
5 - Capriolo (Weissert-OAE)
6 - Polaveno (Weissert-OAE)
7 - Piè del Dosso (OAE1a)
8 - Brasa (T-OAE)
9 - Valle Aviana (Weissert-OAE)
10 - Spiazzi (OAE1a)
11 - Cismon APTICORE (OAE1a)
12 - Cismon (OAE1a, OAE2)
13 - Val del Mis (Wessiert-OAE)
14 - Dogna (T-OAE)
15 - Furlo (OAE2)
16 - Gorgo a Cerbara (OAE1a, OAE2)
17 - Piobbico core (OAE1a)
18 - Monte Petrano (OAE2)
19 - Chiaserna M. Acuto (Weissert-OAE)
20 - Valdorbia (T-OAE)
21 - Colle d'Orlando (T-OAE)
22 - Bottaccione Gorge (OAE2)
23 - Contessa – Gubbio S2 (OAE2)
24 - Contessa (OAE2)
25 - Pozzale (T-OAE)
26 - Somma (T-OAE)
27 - Fonte Cerro (T-OAE)
28 - Coppitella (OAE1a)
29 - Novara di Sicilia (OAE2)
30 - Calabianca (OAE1a, OAE2)
31 - Guidaloca (OAE2)
32 - S'Ozzastru (Weissert-OAE)

Fig. 3

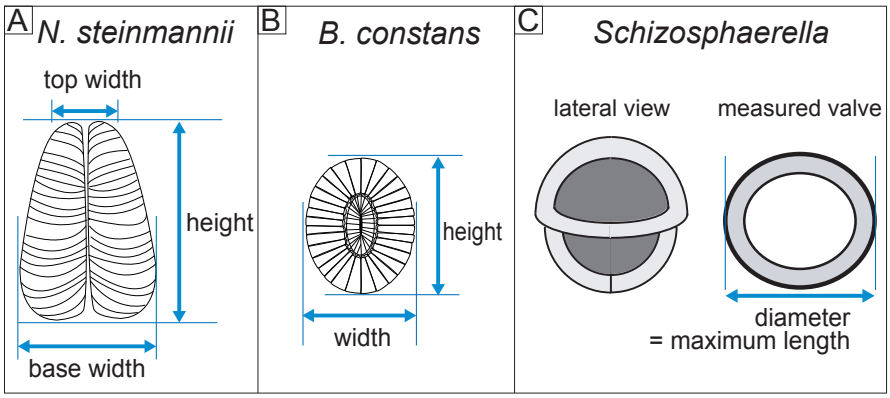

Fig. 4

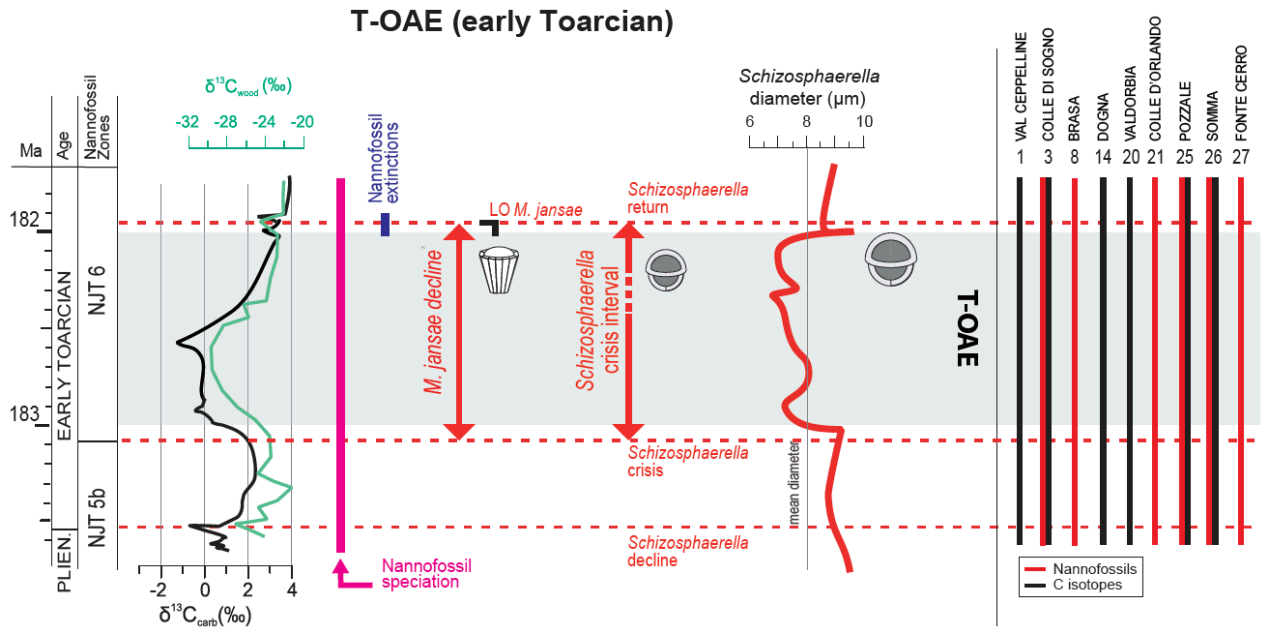
T-OAE (early Toarcian)
Ma
Age
Nannofossil Zones
δ13Cwood (‰)
-32 -28 -24 -20
182
183
EARLY TOARCIAN
NJT 6
NJT 5b
PLIENSB
-2 0 2 4
δ13Ccarb (‰)
Nannofossil extinctions
LO M. jansae
M. jansae decline
Schizosphaerella crisis interval
Schizosphaerella return
Schizosphaerella crisis
Schizosphaerella decline
Nannofossil speciation
Schizosphaerella diameter (µm)
6 8 10
mean diameter
T-OAE
VAL CEPPELLINE 1
COLLE DI SOGNO 3
BRASA 8
DOGNA 14
VALDORBIA 20
COLLE D'ORLANDO 21
POZZALE 25
SOMMA 26
FONTE CERRO 27
Nannofossils
C isotopes

Fig. 5

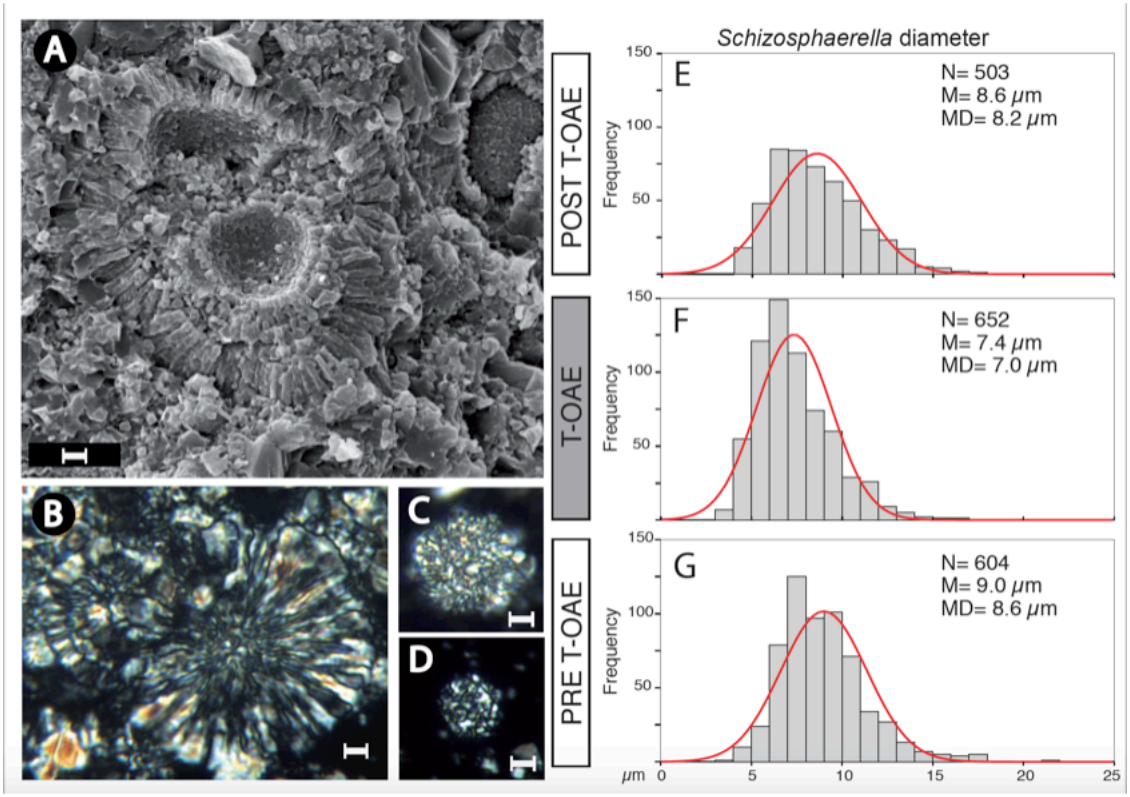
A
B
C
D
POST T-OAE
T-OAE
PRE T-OAE
Schizosphaerella diameter
E
N= 503
M= 8.6 µm
MD= 8.2 µm
F
N= 652
M= 7.4 µm
MD= 7.0 µm
G
N= 604
M= 9.0 µm
MD= 8.6 µm
Frequency
150
100
50
µm 0 5 10 15 20 25

Fig. 6

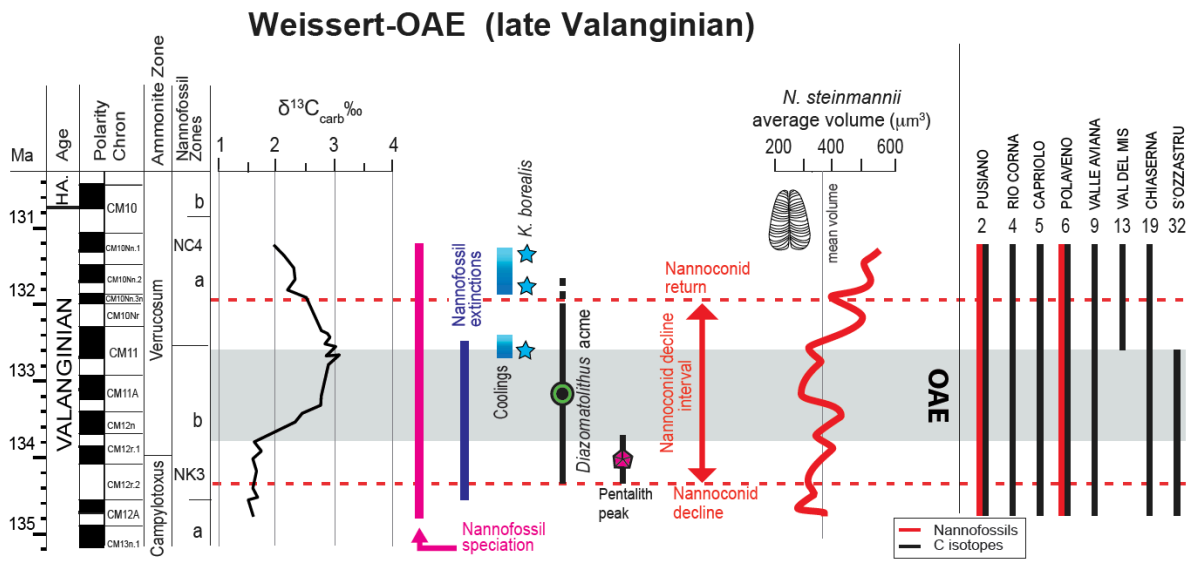
Weissert-OAE (late Valanginian)
Ma
Age
Polarity Chron
Ammonite Zone
Nannofossil Zones
δ13Ccarb ‰
1
2
3
4
N. steinmannii
average volume (μm3)
200
400
600
mean volume
HA.
VALANGINIAN
CM10
CM10Nn.1
CM10Nn.2
CM10Nn.3n
CM10Nr
CM11
CM11A
CM12n
CM12r.1
CM12r.2
CM12A
CM13n.1
Verrucosum
Campylotoxus
b
NC4
a
b
NK3
a
131
132
133
134
135
Nannofossil extinctions
K. borealis
Coolings
Diazomatolithus acme
Pentalith peak
Nannoconid return
Nannoconid decline interval
Nannoconid decline
Nannofossil speciation
OAE
PUSIANO
RIO CORNA
CAPRIOLO
POLAVENO
VALLE AVIANA
VAL DEL MIS
CHIASERNA
S'OZZASTRU
2
4
5
6
9
13
19
32
Nannofossils
C isotopes

Fig. 7

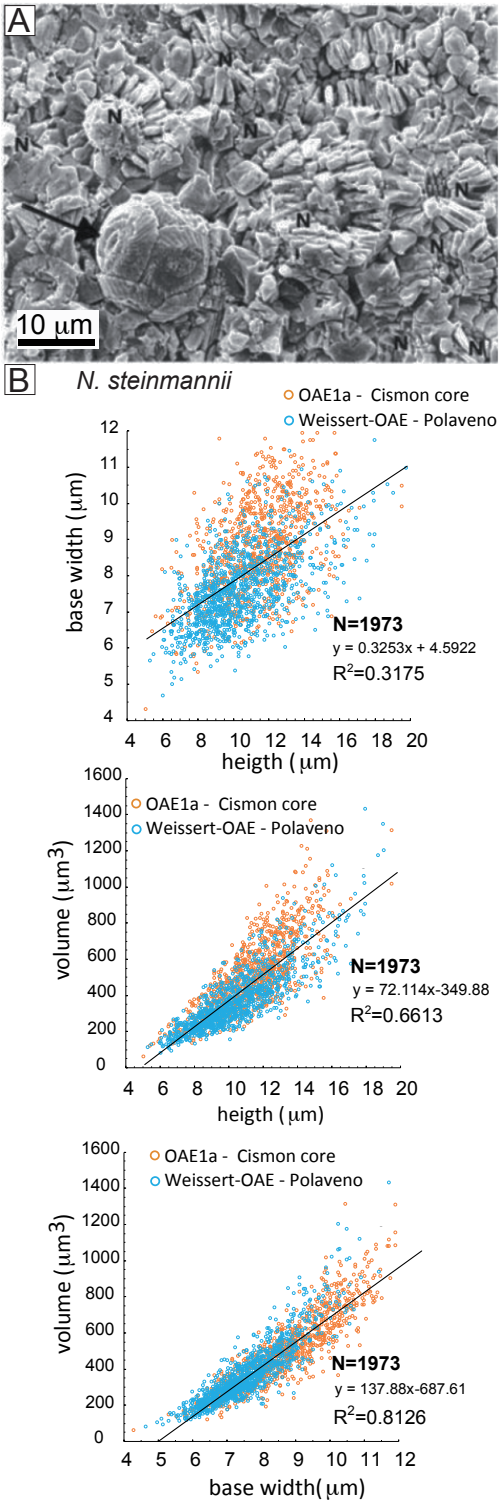
A
10 μm
B
N. steinmannii
OAE1a - Cismon core
Weissert-OAE - Polaveno
base width (μm)
heigth (μm)
N=1973
y = 0.3253x + 4.5922
R2=0.3175
volume (μm3)
heigth (μm)
N=1973
y = 72.114x-349.88
R2=0.6613
volume (μm3)
base width(μm)
N=1973
y = 137.88x-687.61
R2=0.8126

Fig. 8

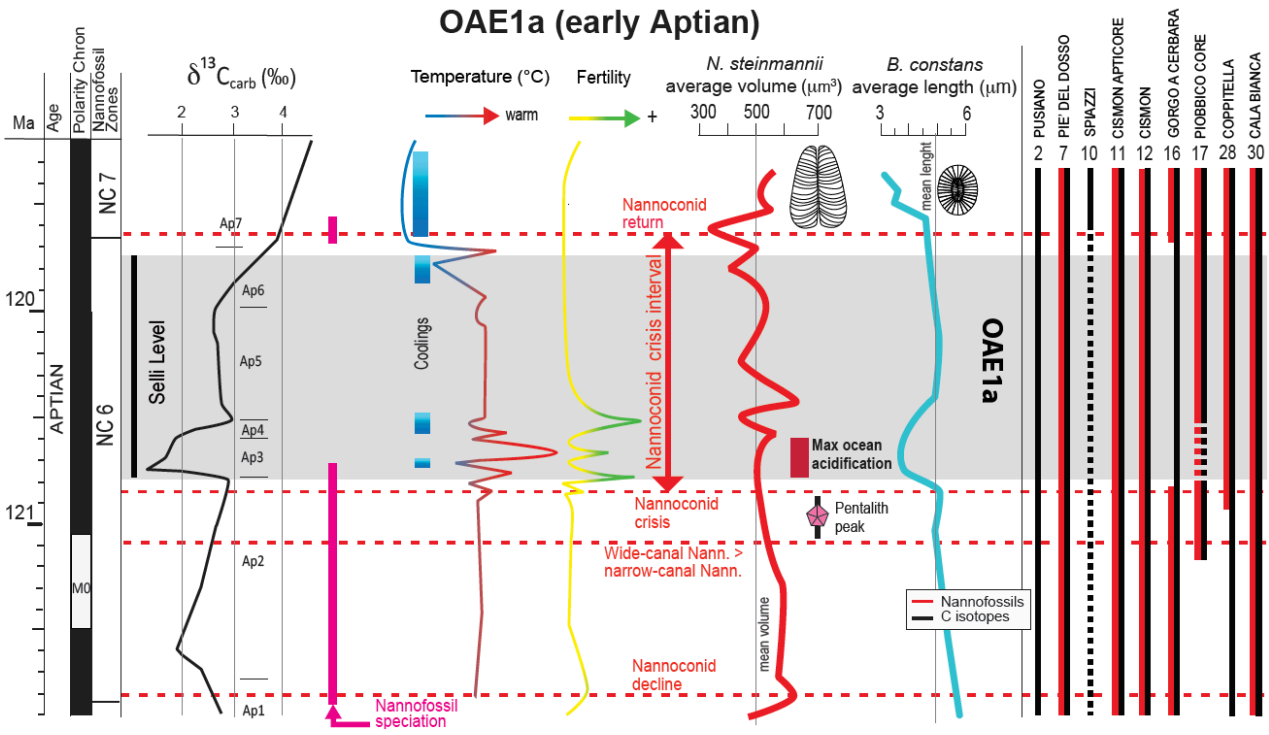
OAE1a (early Aptian)
Ma
Age
Polarity Chron
Nannofossil Zones
δ13Ccarb (‰)
Temperature (°C)
warm
Fertility
N. steinmannii average volume (µm3)
B. constans average length (µm)
mean lenght
PUSIANO
PIE' DEL DOSSO
SPIAZZI
CISMON APTICORE
CISMON
GORGO A CERBARA
PIOBBICO CORE
COPPITELLA
CALA BIANCA
APTIAN
NC 7
NC 6
M0
Ap7
Ap6
Ap5
Ap4
Ap3
Ap2
Ap1
Selli Level
Codings
Nannoconid return
Nannoconid crisis interval
Nannoconid crisis
Wide-canal Nann. > narrow-canal Nann.
Nannoconid decline
Nannofossil speciation
mean volume
Max ocean acidification
Pentalith peak
Nannofossils
C isotopes
OAE1a

Fig. 9

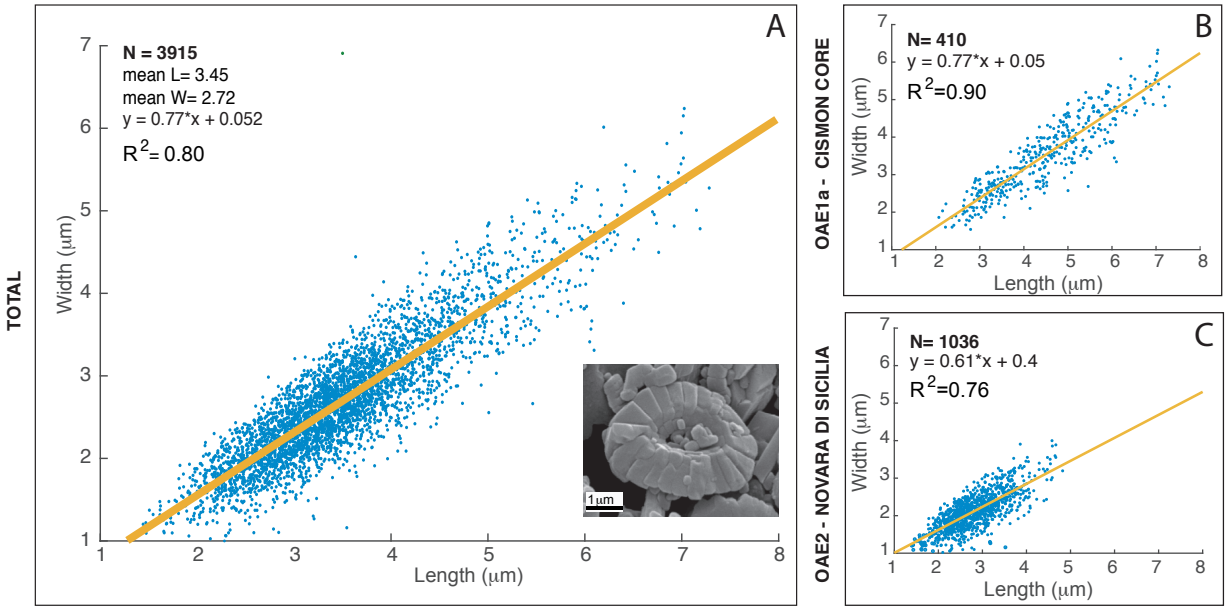
TOTAL
A
N = 3915
mean L= 3.45
mean W= 2.72
y = 0.77*x + 0.052
R2= 0.80
Width (µm)
Length (µm)
1 µm
OAE1a - CISMON CORE
B
N= 410
y = 0.77*x + 0.05
R2=0.90
OAE2 - NOVARA DI SICILIA
C
N= 1036
y = 0.61*x + 0.4
R2=0.76

Fig. 10

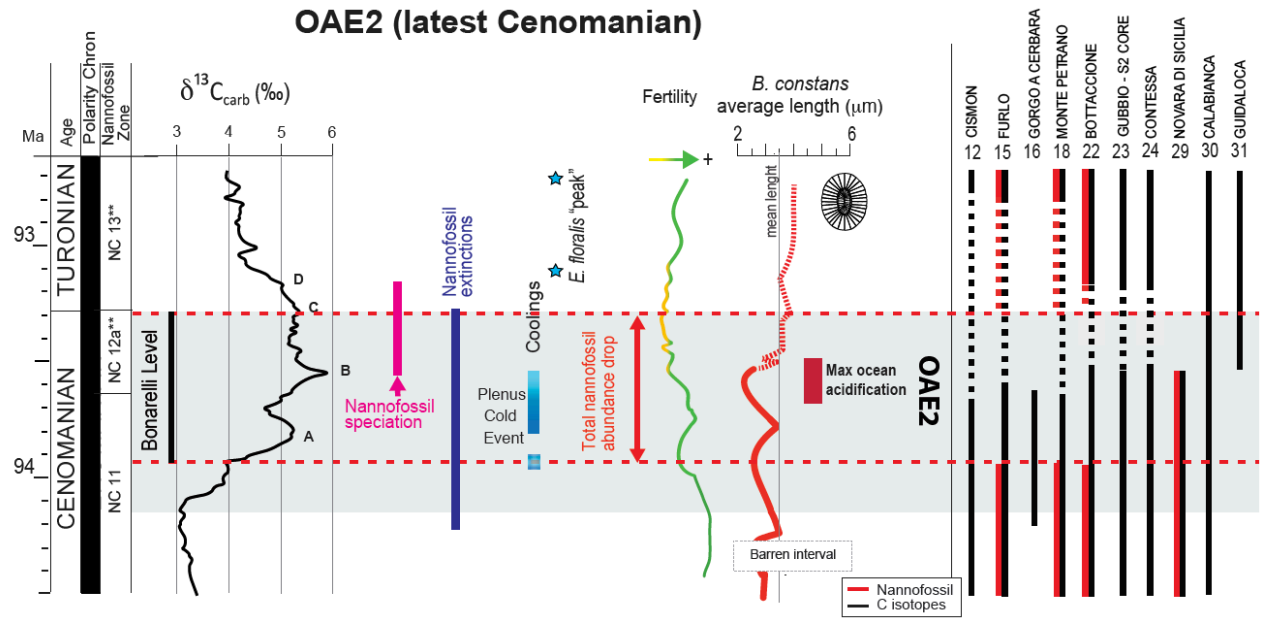

Fig. 11

TABLE 1. ITALIAN PELAGIC SECTIONS WITH NANNOFOSSIL AND CARBON ISOTOPIC DATA FOR T-OAE

n.	Locality	Reference		Nannofossils	$\delta^{13}C$
1.	**Val Ceppelline** (Lombardy Basin, northwestern Italy)	*Jenkyns and Clayton*	*1986*		•
3.	**Colle di Sogno/Mt. Brughetto** (Lombardy basin, northwestern Italy)	*Jenkyns and Clayton*	*1986*		•
		Casellato & Erba	*2015*	•	
8.	**Brasa** (Lombardy Basin, northwestern Italy)	*Cobianchi & Picotti*	*2001*	•	
14.	**Dogna** (Belluno Basin, northeastern Italy)	*Jenkyns et al.*	*2001*		•
20.	**Valdorbia** (Umbria-Marche, central Italy)	*Jenkyns and Clayton*	*1986*		•
		Sabatino et al.	*2009*		•
21.	**Colle d'Orlando** (Umbria-Marche, central Italy)	*Bucefalo Palliani et al.*	*1998*	•	
		Mattioli & Pittet	*2004*	•	
25.	**Pozzale** (Umbria-Marche, central Italy)	*Bucefalo Palliani et al*	*1998*	•	
		Mattioli et al.	*2004b*	•	•
		Mattioli & Pittet	*2004*	•	
26.	**Somma** (Umbria-Marche, central Italy)	*Mattioli & Pittet*	*2002*	•	
		Mattioli et al.	*2004a*	•	
		Mattioli et al.	*2004b*	•	•
		Mattioli et al.	*2009*	•	•
27.	**Fonte Cerro** (Umbria-Marche, central Italy)	*Bucefalo Palliani et al*	*1998*	•	
		Mattioli & Pittet	*2004*	•	

TABLE 2. ITALIAN PELAGIC SECTIONS WITH NANNOFOSSIL AND CARBON ISOTOPIC DATA FOR WEISSERT OAE

n.	Locality	Reference		Nannofossils	$\delta^{13}C$
2.	**Pusiano** (Lombardy Basin, northwestern Italy)	*Channell et al.*	*1993*	●	●
4.	**Rio Corna** (Lombardy Basin, northwestern Italy)	*Lini et al.*	*1992*		●
5.	**Capriolo** (Lombardy Basin, northwestern Italy)	*Lini et al.*	*1992*		●
6.	**Polaveno** (Lombardy Basin, northwestern Italy)	*Lini et al.*	*1992*		●
		Bersezio et al.	*2002*	●	
		Erba & Tremolada	*2004*	●	
		This work		●	
9.	**Valle Aviana** (Trento Plateau, northeastern Italy)	*Lini et al.*	*1992*		●
13.	**Val del Mis** (Belluno Basin, northeastern Italy)	*Channell et al.*	*1993*		●
19	**Chiaserna Monte Acuto** (Umbria-Marche, central Italy)	*Sprovieri et al.*	*2006*		●
32.	**S'Ozzastru** (Sardinia, Italy)	*Bottini et al.*	*2018*		●

TABLE 3. ITALIAN PELAGIC SECTIONS WITH NANNOFOSSIL AND CARBON ISOTOPIC DATA FOR OAE 1A

n.	Locality	Reference		Nannofossils	$\delta^{13}C$
2.	**Pusiano** (Lombardy Basin, northeastern Italy)	*Keller et al.*	*2011*		●
7.	**Piè del Dosso** (Lombardy Basin, northeastern Italy)	*Erba*	*1994*	●	
		Giorgioni et al.	*2015*		●
10.	**Spiazzi** (Trento Plateau, northeastern Italy)	*Weissert et al.*	*1985*		●
11.	**Cismon APTICORE** (Belluno Basin, northeastern Italy)	*Premoli Silva et al.*	*1999*	●	
		Erba et al.	*1999*		●
		Tremolada & Erba	*2002*	●	
		van Breugel et al.	*2007*		●
		Erba & Tremolada	*2004*	●	
		Mehay et al.	*2009*	●	●
		Erba et al.	*2010*	●	●
		Giorgioni et al.	*2015*		●
		Bottini et al.	*2015*	●	
		This work		●	
12.	**Cismon** (Belluno Basin, northeastern Italy)	*Weissert et al.*	*1985*		●
		Erba	*1994*	●	
		Menegatti et al.	*1998*		●
16.	**Gorgo a Cerbara** (Umbria-Marche, central Italy)	*Coccioni et al.*	*1992*	●	
		Erba	*1994*	●	
		Erbacher et al.	*1996*		●
		Tejada et al.	*2009*		●
		Stein et al.	*2011*		●
17.	**Piobbico Core** (Umbria-Marche, central Italy)	*Premoli Silva et al.*	*1989*	●	
		Erba	*1994*	●	
		Erba et al.	*2015*		●
		Bottini et al.	*2015*	●	
28.	**Coppitella** (Gargano, southern Italy)	*Luciani et al.*	*2001*	●	●
30.	**Calabianca** (Sicily, southern Italy)	*Bellanca et al.*	*2002*	●	●

TABLE 4. ITALIAN PELAGIC SECTIONS WITH NANNOFOSSIL AND CARBON ISOTOPIC DATA FOR OAE 2

n.	Locality	Reference		Nannofossils	$\delta^{13}C$
12.	**Cismon** (Belluno Basin, northeastern Italy)	*Gambacorta et al.*	*2015*		●
15.	**Furlo** (Umbria-Marche, central Italy)	*Mort et al.*	*2007*		●
		Jenkyns et al.	*2007*		●
		Gambacorta et al.	*2015*		●
		Bottini & Erba	*2018*	●	
16.	**Gorgo a Cerbara** (Umbria-Marche, central Italy)	*Kuroda et al.*	*2007*		●
18.	**Monte Petrano** (Umbria-Marche, central Italy)	*Erbacher et al.*	*1996*		●
		Gambacorta et al.	*2015*		●
		Bottini & Erba	*2018*	●	
22.	**Bottaccione Gorge** (Umbria-Marche, central Italy)	*Scholle and Arthur*	*1980*		●
		Renard	*1986*		●
		Arthur et al.	*1988*		●
		Corfield et al.	*1991*		●
		Erba	*1994*	●	
		Jenkyns et al.	*1994*		●
		Scopelliti et al.	*2008*		●
		Sprovieri et al.	*2013*		●
23.	**Gubbio - S2 Core** (Umbria-Marche, central Italy)	*Tsikos et al.*	*2004*		●
24.	**Contessa** (Umbria-Marche, central Italy)	*Stoll & Schrag*	*2000*		●
29.	**Novara di Sicilia** (northwestern Sicily, southern Italy)	*Scopelliti et al.*	*2008*		●
		Faucher et al.	*2017*	●	
30.	**Calabianca** (northwestern Sicily, southern Italy)	*Scopelliti et al.*	*2004*		●
		Scopelliti et al.	*2008*		●
31.	**Guidaloca** (northwestern Sicily, southern Italy)	*Scopelliti et al.*	*2004*		●